15. NEOGENE CALCAREOUS NANNOFOSSILS FROM DEEP SEA DRILLING PROJECT SITE 603, LOWER CONTINENTAL RISE, WESTERN NORTH ATLANTIC: BIOSTRATIGRAPHY AND CORRELATIONS WITH MAGNETIC AND SEISMIC STRATIGRAPHY[1]

Jay P. Muza, Sherwood W. Wise, Jr., and J. Mitchener Covington, Florida State University, Tallahassee[2]

ABSTRACT

Calcareous nannofossils are sufficiently numerous in the upper 900 m of the Neogene sediment drift cored beneath the lower continental rise at DSDP Site 603 to permit delineation of zones, correlations with the paleomagnetic data (Pliocene–Pleistocene only), and the detection of major Miocene hiatuses and their correlation with seismic stratigraphy. Holes 603, 603B, and 603C were spudded in lower Pleistocene sediments just east of the crest of the Hatteras Outer Ridge, and all nannofossil zones and subzones are accounted for down to a hiatus within the middle Tortonian (late Miocene) Zone CN8. This hiatus lies some 30 m above a more extensive disconformity between 661 and 672 m where sediments of Subzone CN7a and a portion of Zone CN6 have been removed. The resulting hiatus is correlated with local reflection Horizon M2, which is considered equivalent to the regional Reflector Merlin.

The hiatus between 661 and 672 m dates Merlin at this site between about 9.6 and 10.4 Ma. A strong, parallel, unnamed reflector is correlated with the superjacent hiatus within CN8, and is dated between 8.5 and 9 Ma. These disconformities help delineate a "condensed" interval, which falls within the Vail et al. (1980) cycle TM3.1. This eustatic event has been characterized as the sharpest and most profound sea-level drop of the late Miocene.

The lower Tortonian "condensed" interval at Site 603 is closely correlative with spectacular debris flows cored in presumed canyon fill deposits immediately above reflection Horizon M2/Merlin at DSDP Site 604 on the upper rise off New Jersey. We suggest that the erosion along the lower rise at Site 603 and the synchronous canyon cutting evidenced by the debris flows on the upper rise at Site 604, both associated with the regional Reflector Merlin, are linked closely to Southern Hemisphere glacial activity which led to the formation of the West Antarctic Ice Sheet.

Apart from the lower Tortonian "condensed" interval, the drift sediments of the Hatteras Outer Ridge are primarily muddy contourites, augmented to some extent by fine turbidites in the lower portion. Most were deposited at a rate of about 87 m/Ma. Just after the late Miocene erosional events, sedimentation rates during nannofossil Zone CN8b time were 192 m/Ma, about double that for the overlying section. This suggests that the site was then the locus of deposition for material eroded during canyon-cutting events along the slope and shelf.

The lowest sample dated (911 m) is assigned to Subzone CN5b (not older than 13.1 Ma). A rare glauconitic silty sand turbidite at 834.8 m contains upper Eocene coccoliths, probably eroded from submarine outcrops along the slope, perhaps during a brief middle Miocene canyon-cutting episode.

INTRODUCTION

Deep Sea Drilling Project Leg 93 cored three holes at reentry Site 603 on the lower continental rise 270 mi east of Cape Hatteras, North Carolina (Fig. 1). Each of these recovered sediment from the Hatteras Outer Ridge (HOR), a large Neogene sediment drift which underlies the lower continental rise hills. Age dating these sediments is of interest because North Atlantic drift deposits such as this record marked changes in the nature of abyssal circulation which, in turn, reflect important steps in the evolution of the North Atlantic Basin and the development of glacial climates. We discuss here the calcareous nannofossil biostratigraphy and its relationship to the magnetic and seismic stratigraphy of the Neogene sediments of the HOR recovered at Site 603.

Site 603 was located in the first trough seaward of the crest of the HOR, which at this locality separates a turbidite pond to the west from the lower continental rise hills to the east (Fig. 2). The sediments were sampled in three phases. An exploratory hole (Hole 603) was washed and spot cored down to 573 m, continuously cored to 803 m, then washed and rotary cored to 833 m. Following an unsuccessful attempt to set a reentry cone, reentry Hole 603B was washed and drilled down to 821 m, washed and rotary cored over short intervals to 927 m, then continuously cored to a total depth of 1585.2 m. Hole 603C was then continuously cored from the surface down to 91 m using the hydraulic piston corer (HPC), then cored down to 366 m using the extended core barrel (XCB).

The Neogene sediments are assigned to lithostratigraphic Unit I (Fig. 3), which consists of 960 m of lower or middle Miocene to lower Pleistocene hemipelagic clay and claystone (Blake Ridge Formation of Jansa et al., 1979). This unit is further subdivided on the basis of lithology and color into four subunits (Fig. 3). The dark green homogeneous muds (muddy contourites) of Subunit IA contain coccoliths and planktonic foraminifers deposited above the calcite compensation depth. Greenish gray muds of Subunits IB and IC are largely devoid of calcareous microfossils except for the more dissolution resistant discoasters and, in the lower part of Subunit IB, isolated coccolith-rich intervals that yield 10 to 20% nannofossils. Subunit IC contains appreciable num-

[1] van Hinte, J. E., Wise, S. W., Jr., et al., *Init. Repts. DSDP*, 93: Washington (U.S. Govt. Printing Office).

[2] Addresses: (Muza) Department of Oceanography, Florida State University, Tallahassee, Florida 32306; (Wise) Department of Geology, Florida State University, Tallahassee, Florida 32306; (Covington, present address) Texaco USA, P.O. Box 60252, New Orleans, LA 70160.

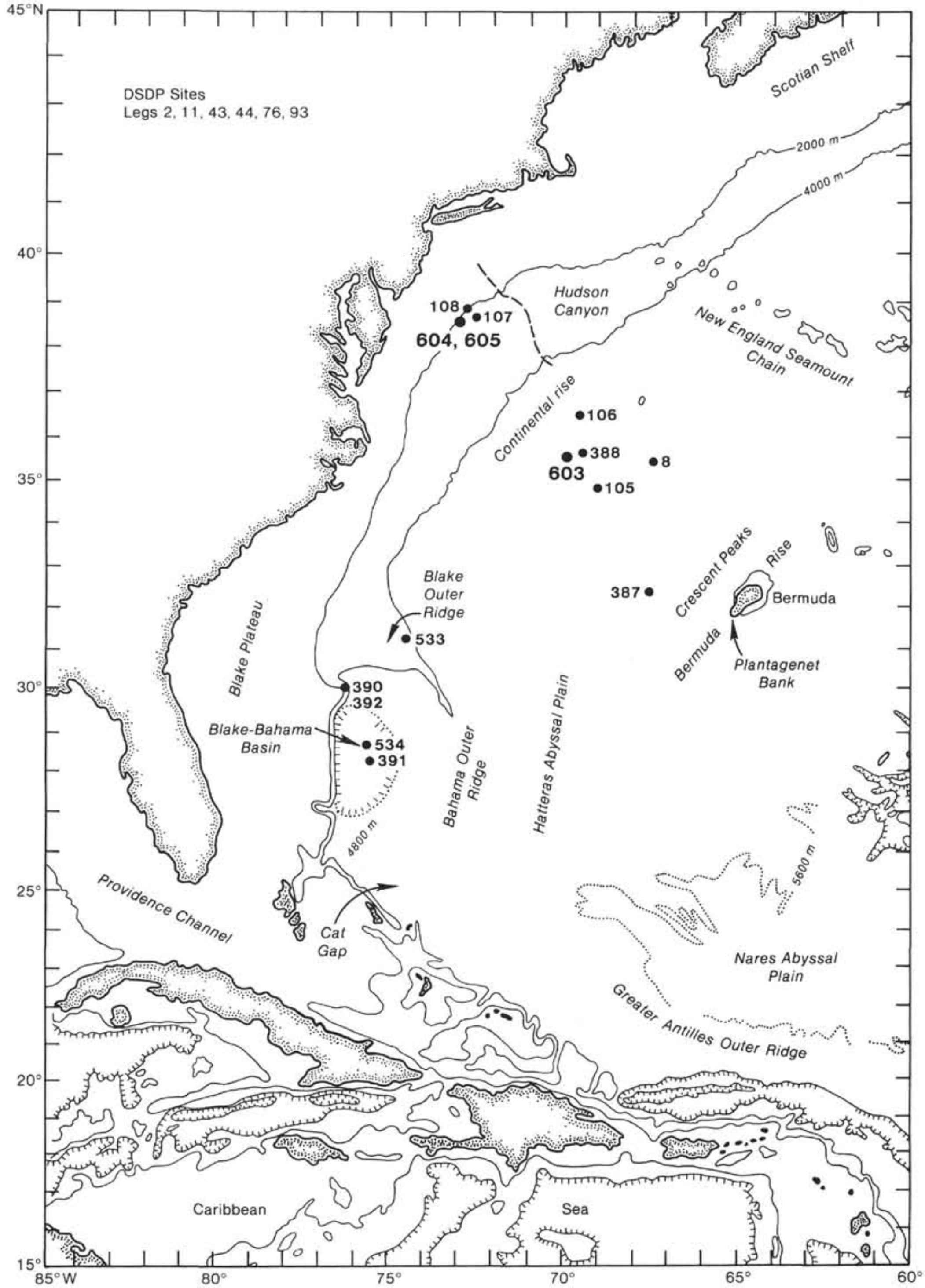

Figure 1. Location of DSDP Site 603 and other selected DSDP sites in the western North Atlantic.

bers of radiolarians at various intervals as well as the first unambiguous evidence of sporadic silt and sand turbidites below 720 m. Subunit IC is essentially barren of coccoliths below 936 m. In contrast to the green clays above, Subunit ID is composed of yellowish brown to brown clays that are barren of microfossils except for fish teeth, which Hart and Mountain (this volume) dated as early to middle Miocene in age.

We describe the nannofossil assemblages from the top of the section down. Hole 603C provided the most complete and highest quality recovery for the top of the section, where coccoliths were also the most numerous and best preserved. Therefore, this hole will be described first and in the most detail. The overlapping Hole 603 will be discussed next, followed by Hole 603B, which recovered the base of lithostratigraphic Unit I.

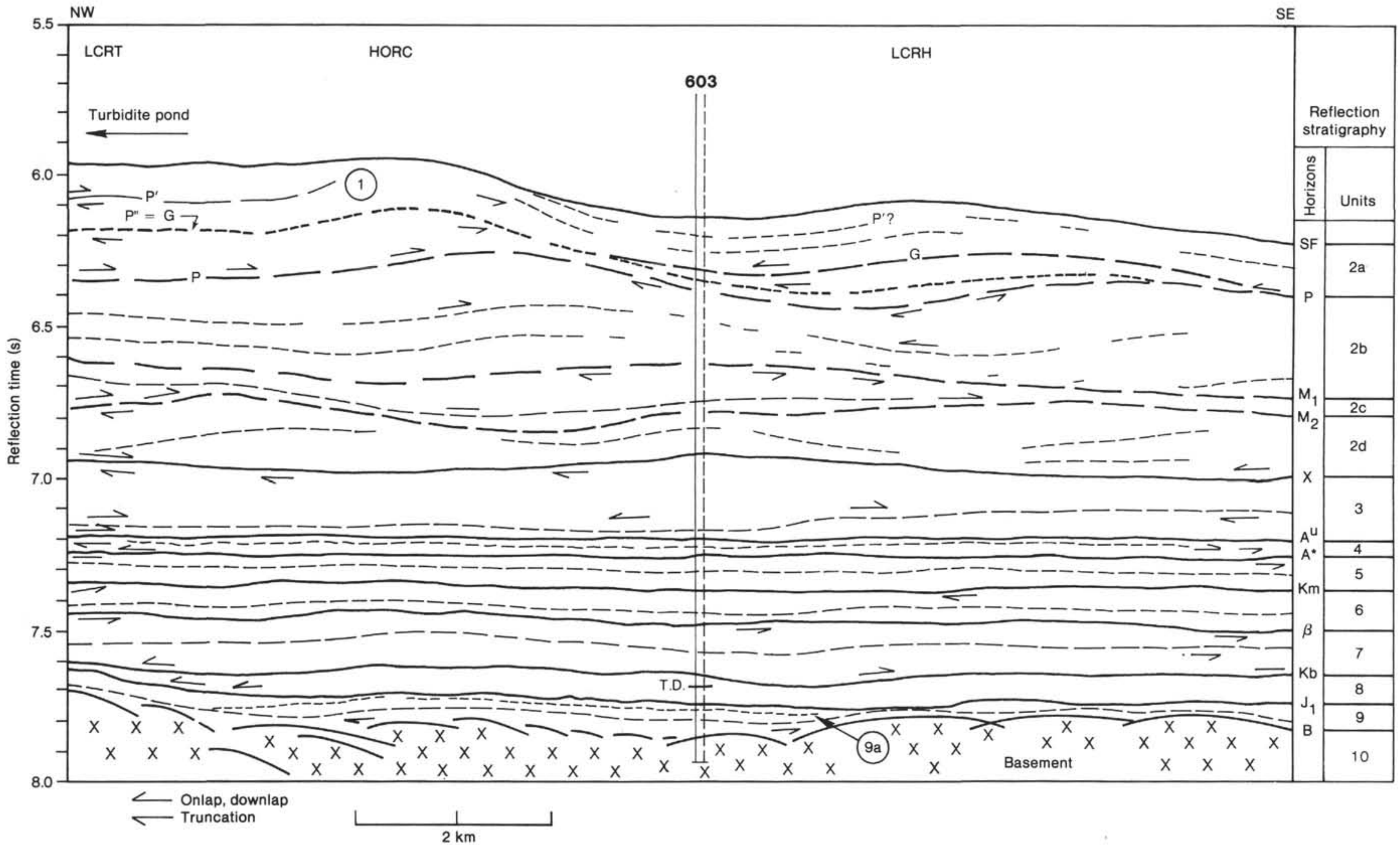

Figure 2. Line drawing after multichannel seismic reflection profile Conrad 2101, line 77 showing location of DSDP Site 603. LCRT = lower continental rise terrace; HORC = Hatteras Outer Ridge Crest; LCRH = lower continental rise hills.

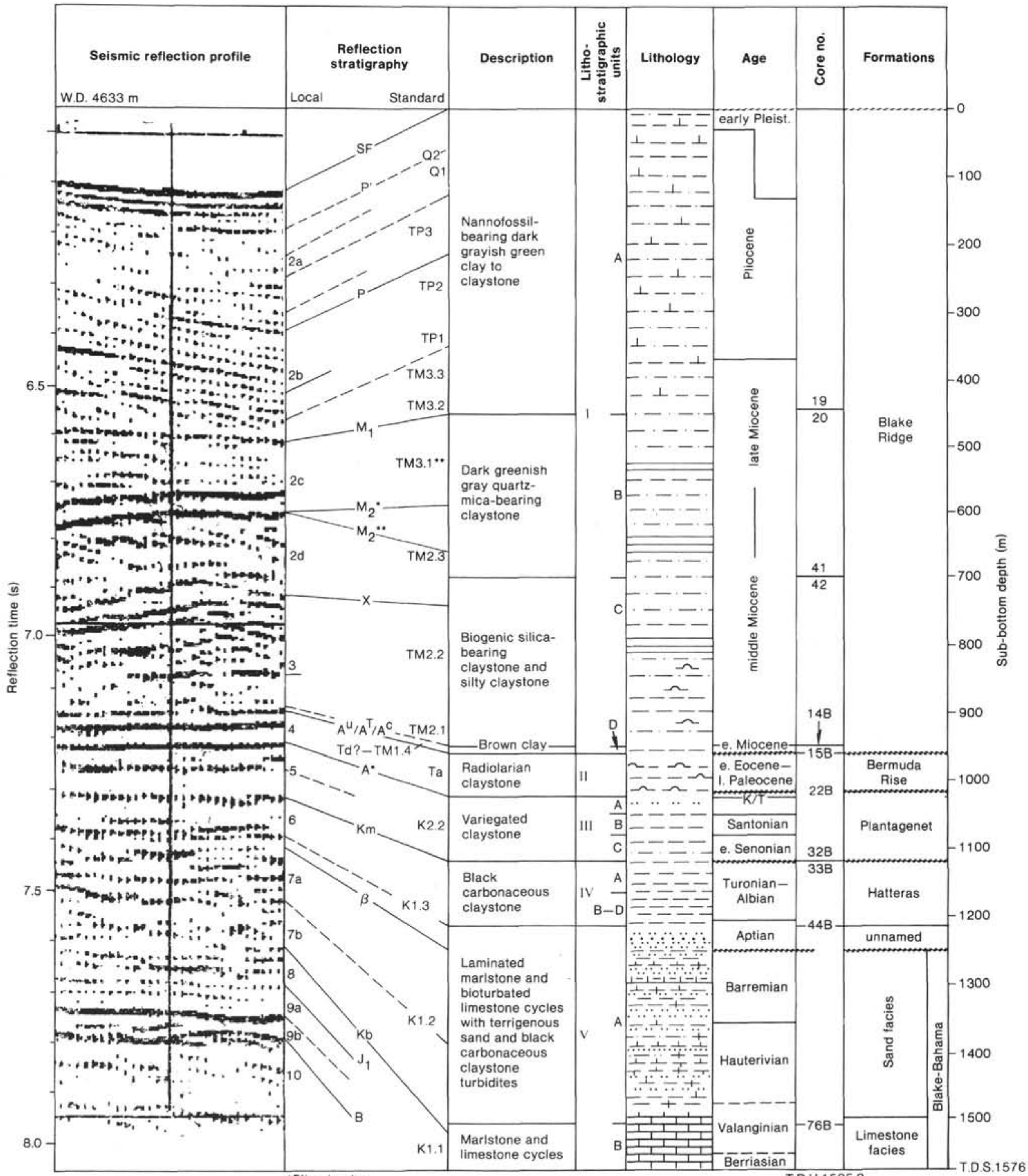

Figure 3. Stratigraphic summary of Site 603 (Holes 603 to 603C). Units I–V are local lithostratigraphic units; Units 1–10 are local seismostratigraphic units; standard seismic sequence notation after Vail et al. (1980).

METHODS, ZONATION, AND SPECIES CONSIDERED

The nannofossil assemblages were described from smear slides made from samples which, for Hole 603C, were taken at an interval of at least 1 sample per section. For Holes 603 and 603B, where coccoliths were less common, we also examined at least one sample per core section. We selected from these and plotted on the distribution charts, however, only the most fossiliferous sample found in each core. Smear slides were made directly from the raw sediment sample and examined at a magnification of 1000×. Estimates of the abundances of individual nannofossil species on the smear slides were tabulated on range charts using the method of Hay (1970). Letters used to denote abundances are keyed to the ^{10}log of the number of specimens of a taxon likely to be observed in any one field of view of the microscope. These and the corresponding logs are determined as follows:

H = Highly abundant, +2 (more than 100 specimens per field of view)
V = Very abundant, +1 (more than 10 specimens per field of view)
A = Abundant, 0 (1 to 10 specimens per field of view)
C = Common, −1 (1 specimen per 2 to 10 fields of view)
F = Few, −2 (1 specimen per 11 to 100 fields of view)
R = Rare, −3 (1 specimen per 101 to 1000 fields of view)

Through visual inspection at 1000×, a qualitative determination was made of the state of preservation of the nannofossils in each sample. In any given sample, the state of preservation may be different for each individual species, genus, or morphologic group. For example, discoasters may exhibit calcite overgrowths, whereas in the same sample, the placoliths may appear to be etched or may be absent through selective dissolution. Thus, any qualitative measurement of a given sample must be based on the overall preservational qualities of the nannofossil assemblage. The following basic criteria were used to qualitatively describe the degree of preservation, dissolution, or overgrowth of a nannofossil assemblage:

G = Good: individual specimens exhibit no dissolution or recrystallization.
M = Moderate: individual specimens yield slight evidence of dissolution (etching) and/or recrystallization (overgrowths).
P = Poor: individual specimens exhibit considerable dissolution and/or recrystallization; placoliths dissolved and ragged; some discoasters overgrown, making species determination difficult, if not impossible.

The Site 603 assemblages ranged from good to poor preservation, with the majority of assemblages exhibiting moderate preservation.

In an effort to maximize the Neogene biostratigraphic resolution at Site 603, the calcareous nannofossil schemes of Gartner (1977) and Okada and Bukry (1980) were combined (Fig. 4). The Pleistocene zonation is from Gartner (1977) and the Pliocene and Miocene zonations are from Okada and Bukry (1980). Since both zonal schemes base the Pliocene/Pleistocene boundary on the LAD of *Discoaster brouweri*, the combined scheme used in this paper is continuous. One should note that Okada and Bukry's CN12d has recently been renamed the *D. triradiatus* Subzone (Bukry, 1985, p. 572) to avoid confusion when the two systems are combined. One should also note that we have changed the name of the *D. pentaradiatus* Subzone (CN12c) to the *D. misconceptus* Subzone in order to conform with the nomenclatural changes proposed by Theodoridis (1984).

Taxa considered in this chapter are listed in an appendix, where they are arranged alphabetically by specific epithets. Bibliographic references for these species are given in Loeblich and Tappan (1966, 1968, 1969, 1970a, b, 1971, 1973), van Heck (1979a, b, 1980a, b, 1982), or Steinmetz (1985). Remarks on taxonomic concepts and one new combination are given under "Taxonomic Notes" near the end of the narrative.

As noted in the Introduction, both wash and rotary cores were taken at Holes 603 and 603B. Rotary cores are the standard cores cut over a 9.6-m interval and retrieved before further penetration. Wash cores, labeled "M" in the Site 603 chapter, are obtained over intervals longer than 9.6 m by leaving the core barrel in place while drilling or washing ahead. One cannot specify where in the interval penetrated the sediment in the core barrel came from. By convention, any sediment recovered is measured from the top of the interval.

HOLE SUMMARIES

Hole 603C (Table 1)

Hole 603C (35°29.78′N; 70°01.86′W; water depth 4643 m) was spudded into lower Pleistocene sediment. Sample 603C-1-1, top, to Sample 603C-2-3, 30–32 cm contains an abundant, well-preserved assemblage that belongs to the *Helicosphaera sellii* Zone (Gartner, 1977). Species dominant in this interval are *Pseudoemiliania lacunosa, H. sellii, H. carteri, Calcidiscus leptoporus, Coccolithus pelagicus, Gephyrocapsa* spp. and *Reticulofenestra haqii.*

The *Calcidiscus macintyrei* Zone (Gartner, 1977) extends from Sample 603C-2-4, 30–32 cm to Sample 603C-4-5, 30–32 cm. Species dominant in this well-preserved assemblage include *C. macintyrei, Ceratolithus cristatus*, and *H. carteri* as well as those species listed for the overlying zone. Reworked Upper Cretaceous microfossils are common in this interval, particularly in Cores 3 and 4. This reworked Cretaceous assemblage includes *Eiffellithus eximius, E. turriseiffeli, Uniplanarius gothicus, Zygodiscus* sp., and *Micrantholithus* sp.

The Pliocene/Pleistocene boundary is present in Section 603C-4-5 between 32 and 110 cm, based on the last occurrence datum (LOD) of *Discoaster brouweri*. The *D. brouweri* Zone (CN12) consists of four subzones which are all present in the cored interval from Hole 603C.

The *D. triradiatus* Subzone (CN12d) is present from Sample 603C-4-5, 110 cm to Sample 603C-9-4, 30–32 cm. Species dominant in this well-preserved interval include *Ceratolithus cristatus, Calcidiscus leptoporus, C. macintyrei, H. sellii, H. carteri, P. lacunosa, Pontosphaera* spp., *R. haqii, Gephyrocapsa* spp., *Coccolithus pelagicus, D. brouweri*, and *D. triradiatus.*

Extending from Sample 603C-9-5, 30–32 cm to Sample 603C-10-4, 30–32 cm is the *D. misconceptus* Subzone (CN12c) (= *D. pentaradiatus* Subzone of Okada and Bukry, 1980). This assemblage is differentiated from the overlying assemblage of CN12d only by the added presence of *D. misconceptus* (Theodoridis, 1984) Muza and Wise, n. comb. (= *D. pentaradiatus* of the pre-1985 literature).

Preservation is good and abundances are high between Samples 603C-10-5, 110–112 cm and 603C-13-1, 30–32 cm. This interval is representative of the *D. surculus* Subzone (CN12b). Species prevalent here include *D. surculus, D. brouweri, D. misconceptus, P. lacunosa, H. sellii, Calcidiscus macintyrei, C. leptoporus, Coccolithus pelagicus, R. haqii, Pontosphaera* spp., *D. triradiatus, Ceratolithus cristatus, Syracosphaera* sp. and *Scyphosphaera* spp.

The interval from Sample 603C-13-2, 30–32 cm to Sample 603C-21-7, 30–32 cm, is placed in the *D. tamalis* Subzone (CN12a). Nannofossil preservation in this zone is poor to good, and specimens are common to abundant. Species prevalent in this interval are similar to those in Subzone CN12b above, with the added presence of *D. tamalis, D. asymmetricus*, and *D. variabilis*. Intervals of high dissolution that may represent an elevated CCD are prevalent in Core 15.

The *R. pseudoumbilica* Zone (CN11) can be divided into two subzones (CN11b and CN11a) which are both present in Hole 603C. The LOD of *Sphenolithus* sp. defines the top of the *R. pseudoumbilica* Zone and the *D. asymmetricus* Subzone (CN11b). The *D. asymmetricus* Subzone is present from Sample 603C-22-1, 30–32 cm to Sample 603C-25-2, 30–32 cm. Preservation in this interval is poor to moderate, becoming increasingly better downcore. Prevalent species in this interval include those found in the overlying CN12a interval with the addition

Age	Zone		Subzone		Datum
late Pleistocene	*Emiliania huxleyi* acme				FOD *E. huxleyi* acme
	Emiliania huxleyi				FOD *E. huxleyi*
	Gephyrocapsa oceanica				LOD *P. lacunosa*
early Pleistocene	*Pseudoemiliania lacunosa*				Highest level of dominantly small *Gephyrocapsa*
	small *Gephyrocapsa*				LOD *H. sellii*
	Helicosphaera sellii				LOD *C. macintyrei*
	Calcidiscus macintyrei				LOD *D. brouweri*
late Pliocene	CN12	*Discoaster brouweri*	CN12d	*Discoaster triradiatus*	LOD *D. pentaradiatus*
			CN12c	*Discoaster misconceptus*	LOD *D. surculus*
			CN12b	*Discoaster surculus*	LOD *D. tamalis*
			CN12a	*Discoaster tamalis*	LOD *R. pseudoumbilica* or LOD *Sphenolithus* spp.
early Pliocene	CN11	*Reticulofenestra pseudoumbilica*	CN11b	*Discoaster asymmetricus*	FOD *D. asymmetricus* acme
			CN11a	*Sphenolithus neoabies*	LOD *A. primus* or LOD *A. tricorniculatus*
	CN10	*Amaurolithus tricorniculatus*	CN10c	*Ceratolithus rugosus*	FOD *C. rugosus* or LOD *C. acutus*
			CN10b	*Ceratolithus acutus*	FOD *C. acutus* or LOD *T. rugosus*
			CN10a	*Triquetrorhabdulus rugosus*	LOD *D. quinqueramus*
late Miocene	CN9	*Discoaster quinqueramus*	CN9b	*Amaurolithus primus*	FOD *A. primus* or FOD *A. delicatus*
			CN9a	*Discoaster berggrenii*	FOD *D. berggrenii* or FOD *D. surculus*
	CN8	*Discoaster neohamatus*	CN8b	*Discoaster neorectus*	FOD *D. neorectus* or FOD *D. loeblichii*
			CN8a	*Discoaster bellus*	LOD *D. hamatus*
	CN7	*Discoaster hamatus*	CN7b	*Catinaster calyculus*	FOD *C. calyculus*
			CN7a	*Helicosphaera carteri*	FOD *D. hamatus*
middle Miocene	CN6	*Catinaster coalitus*			FOD *C. coalitus*
	CN5	*Discoaster exilis*	CN5b	*Discoaster kugleri*	FOD *D. kugleri*
			CN5a	*Coccolithus miopelagicus*	LOD *S. heteromorphus*

Figure 4. Zonal scheme used in this paper, adopted from Gartner (1977) and Gartner et al. (1984), Okada and Bukry (1980), with markers originally defined in Bukry (1973, 1975). FOD = first occurrence datum; LOD = last occurrence datum.

of *Sphenolithus abies, S. neoabies*, and *R. pseudoumbilica*.

The top of Subzone CN11a, the *S. neoabies* Subzone, is recognized by the beginning of the acme of *D. asymmetricus*. The better preservation in the lower part of the *R. pseudoumbilica* Zone may be responsible for the downhole increase in abundance of *D. asymmetricus* between Samples 603C-23-7, 30–32 cm and 603-25-2, 30–32 cm. *D. asymmetricus* also increases drastically in abundance in Sample 603C-23-1, 30–32 cm, where preservation is noticeably improved. On the basis of the better preserved samples, therefore, the *S. neoabies* Subzone (CN11a) is recognized from Samples 603C-25-3, 30–32 cm to 603C-30-2, 30–32 cm.

The *Amaurolithus tricorniculatus* Zone (CN10) is present from Samples 603C-30,CC to 603C-36-5, 30–32 cm. It is possible to separate this interval into its three subzones.

The *Ceratolithus rugosus* Subzone (CN10c) is present from Samples 603C-30,CC to 603C-33-6, 30–32 cm. Sample 603C-33,CC is barren.

The *C. acutus* Subzone (CN10b) is recognized in Sample 603C-34-1, 40–42 cm, the only sample in which *C. acutus* was observed. Unfortunately, in Core 603C-34 only 120 cm of sediment plus the core-catcher sample were recovered. Thus, Subzone CN10b extends to some point between 603C-34-1, 40-42 cm and 603C-34,CC, where the LO of *Triquetrorhabdulus rugosus* is observed.

The *T. rugosus* Subzone (CN10a) is observed in the interval from Samples 603C-34,CC through 603C-36-5, 30–32 cm.

Preservation throughout the entire *A. tricorniculatus* Zone is marked by moderate, poor, and barren intervals. Overgrown discoasters and etched placoliths are common in this interval. Nannofossils are generally not so abundant, by at least an order of magnitude, as those observed upsection, and many intervals are barren of all calcareous microfossils.

The *Discoaster quinqueramus* Zone (CN9) is present from Sample 603C-36-6, 30–32 cm to the base of the hole (Sample 603C-40,CC). Preservation is moderate to poor and nannofossil abundances are much the same as in Zone CN10. Species which dominate this interval are *T. rugosus, R. haqii, R. pseudoumbilica, S. abies, S. neoabies, D. surculus, D. quinqueramus, D. misconceptus, D. brouweri, D. variabilis*, and *Calcidiscus leptoporus. A. primus, H. sellii*, and *C. macintyrei* are generally present but to a lesser degree.

The absence of *A. primus* from Sample 603C-39,CC to the bottom of the hole (366.0 m) at first glance might suggest that Samples from this interval should be placed in the *D. berggrenii* Subzone (CN9a). It should be noted, however, that *A. primus* occurs rather sporadically from Cores 603C-37 to -39, and that *A. delicatus* is recorded in Sample 603C-40-4, 30–32 cm. As will be discussed later for Hole 603, the first occurrence (FO) of *A. delicatus* occurs at 462 m, well below the total depth of Hole 603C. According to Gartner and Bukry (1975), the FOD of *A. delicatus* is slightly above that of *A. primus*, a fact confirmed for the mid-latitude North Atlantic at DSDP Site 558A by Parker et al. (1985). This would indicate that Hole 603C bottomed out in the *A. primus* Subzone (CN9b) rather than in the *D. berggrenii* Subzone (CN9a).

Preservation below 603C-39,CC is poor; because of overgrowth and excessive breakage, the six-rayed discoasters generally cannot be readily identified at the species level. Six-rayed discoasters are, however, relatively abundant, as are *R. haqii, C. leptoporus, C. pelagicus, S. abies, S. neoabies, R. pseudoumbilica, D. berggrenii, D. quinqueramus*, and *D. variabilis*.

The nannofossil Miocene/Pliocene boundary is picked here on the extinction of *D. quinqueramus*. Coccolith specialists do not all accept this pick nor do they all correlate this datum to the same level in the paleomagnetic time scale. Our pick, however, when correlated with the magnetic stratigraphy of Hole 603C, seems to confirm the correlation of Gartner et al. (1984), who place the extinction of *D. quinqueramus* within the lower Gilbert (see discussion later under "Hole 603C: Correlations with Magnetostratigraphy").

Hole 603 (Table 2)

Hole 603 (35°29.66′N; 70°01.70′W; water depth 4634.0 m) is located some 300 m east-southeast of Holes 603B and 603C. Diversity is relatively high in Cores 603-1 to -19, reflecting deposition significantly above the CCD. Preservation there is generally moderate to good. Relatively low diversity, zones barren of calcareous microfossils, and poor to moderate preservation in Cores 603-20 to -54 reflect deposition near a fluctuating CCD.

The nearly continuous Pliocene and Pleistocene section is represented by Cores 603-1 to -15. The assemblages are essentially the same as those in equivalent strata in Hole 603C, but the intervals they represent are less certain because of the large number of wash cores taken. The sediment in a washed core could come from anywhere within the washed interval, although it is probable that the core barrel is filled in the upper portion of the interval. Because of the uncertainty, however, we do not include the first 15 cores on the range chart (Table 2), but we do provide a written description of the assemblages.

Core 603-1 contains abundant *Gephyrocapsa* spp., *Pseudoemiliania lacunosa, Calcidiscus leptoporus*, relatively common *Helicosphaera sellii*, and a few *Ceratolithus cristatus*. This assemblage is assigned to the early Pleistocene *H. sellii* Zone of Gartner (1977).

Core 603-2M (M = wash core) contains abundant *Discoaster brouweri* in addition to those species mentioned in Core 603-1. Core 603-2M belongs to the Pliocene *D. brouweri* Zone (CN12), which is not further subdivided here because this was a wash core accumulated over a hole distance of 75 m.

Cores 603-3M through -7M belong to the *D. tamalis* Subzone (CN12a) of the *D. brouweri* Zone. Species generally common to abundant in these cores include *D. tamalis, D. brouweri, D. asymmetricus, D. misconceptus, D. surculus, H. sellii, C. cristatus, Calcidiscus macintyrei*, and *P. lacunosa*. Core 603-6 had no sediment recovery.

Rotary Cores 603-8 through -10 contain an assemblage similar to the above plus generally common to abundant *Reticulofenestra pseudoumbilica* and the LO of *Sphenolithus* spp. in Section 603-9-2. Thus, these cores can be assigned to the *D. asymmetricus* Subzone (CN11b) of the *Reticulofenestra pseudoumbilica* Zone (CN11).

The common occurrences of *R. pseudoumbilica, D. misconceptus, D. surculus, Sphenolithus* spp., *Amaurolithus delicatus, Ceratolithus cristatus* (= *C. rugosus*), *Calcidiscus macintyrei*, and *P. lacunosa*, as in Core 603-11M, place Cores 603-12 and 13 in the *Ceratolithus rugosus* Subzone (CN10c).

The *C. acutus* Subzone (CN10b) is recognized in the gap between the LO of *Triquetrorhabdulus rugosus* (603-14-4) and the FO of *C. cristatus* or *C. rugosus. C. acutus* was not observed, however, and the location of the FO of *C. cristatus* is uncertain because the exact position of the cored material within the 38.4-m washed interval of Core 603-13M is unknown. The LO of *T. rugosus* in Section 4 of Core 603-14 is only tentatively placed there, and *C. acutus* was not found. However, *C. acutus* was noted in one sample from an interval of poor recovery in Hole 603C, so that all of the zones and subzones in question are accounted for at this site.

We use the LO of *D. quinqueramus*, in Sample 603-16-1, 100–102 cm to mark the Miocene/Pliocene boundary in this section (see discussion later). Because of the

Table 1. Distribution of Miocene to Pleistocene calcareous nannofossils, DSDP Hole 603C.

Age		Zone/Subzone		Sub-bottom depth (m)	Core-Section (interval in cm)	Relative abundance	Preservation	*Amaurolithus delicatus*	*A. primus*	*A. tricorniculatus*	*Braarudosphaera bigelowii*	*Ceratolithus acutus*	*C. cristatus/telesmus*	*Calcidiscus leptoporus*	*C. macintyrei*	*Coccolithus pelagicus*	*Discoaster asymmetricus*	*D. berggrenii*	*D. brouweri*	*D. intercalaris*	*D. misconceptus*	*D. quinqueramus*	*D. surculus*	*D. tamalis*	*D. triradiatus*	*D. variabilis*	*Discoaster* spp. (overgrown/dissolved)	*Gephyrocapsa* spp.	*Helicosphaera carteri*	*H. sellii*	*Pontosphaera japonica*	*P. multipora*	*Pontosphaera* sp.	*Pseudoemiliania lacunosa*	*Reticulofenestra haqii*	*R. pseudoumbilica*	*Rhabdosphaera* sp.	*Scyphosphaera* sp.	*Syracosphaera* sp.	*Sphenolithus abies*	*S. neoabies*	*Triquetrorhabdulus rugosus*	*Umbilicosphaera cricota*	Reworked species	*Discoaster deflandrei*	*D. loeblichi*	*D. multiradiatus*	*D. saipanensis*	*Isthmolithus recurvus*	Reworked Cretaceous (see text)
Pleistocene	early	*H. sellii*		0.1	1-1, 12	A	G						C	V		A												H	A	A		C		C	V		C						A							
				—	1,CC	A	G																					H	A	A		C		C	V		C						C							
				2.3	2-1, 30-32	A	G						C	V		A												H	A	A		C		V	V		C						C							
				3.8	2-2, 30-32	A	G						F	V		A												H	A	A			A	V	V		C													
				5.3	2-3, 30-32	A	G						C	A		A			r					r				H	A	A			A	V	V			R				r								
		C. macintyrei		6.8	2-4, 30-32	A	G						C	A	C	A												H	A	A			A	A	V								C							
				8.3	2-5, 30-32	A	G						C	A	A	V												V	A	A			C	V	V								F							
				9.8	2-6, 30-32	A	G						C	A	A	A									c	f		H	A	A			A	V	V		C						F							
				11.9	3-1, 30-32	A	G						C	C	C	A												V	C	C			A	A	V		C	F												a
				13.4	3-2, 30-32	A	G						C	A	A	C												A	A	C		F		A	V								F							c
				14.9	3-3, 30-32	A	M						C	A	A	C			r									A	A			F		V	V															c
				16.4	3-4, 30-32	A	M						C	A	A	C												V	A	C		A		A	V															a
				17.9	3-5, 30-32	A	G						C	A	A	A												V	A	C		A		V	V		A	A												a
				19.4	3-6, 30-32	A	G						C	A	A	A												V	A	A		A		V	V		C													a
				20.9	3-7, 30-32	A	G						C	A	A	C												V	A	A		F		V	V		C	F												a
				21.5	4-1, 30-32	A	G						C	A	A	A												A	A	C		A		A	V			R												
				23.0	4-2, 30-32	A	G						C	A	A	A			r									V	A	A		C		A	V		C	F	F											
				24.5	4-3, 30-32	A	G						F	A	C	A			r					r				V	A	A			A	A	V			F	C				F							
				26.0	4-4, 30-32	A	G						C	A	A	A												V	A	A			A	A	A		C	F	C				A							
				27.5	4-5, 30-32	A	G						C	A	A	A			f		r				f			V	A	A			C	A	V		C		C				A							
Pliocene	late	*D. brouweri* (CN12)	*D. triradiatus* (CN12d)	29.0	4-6, 30-32	A	G						C	A	A	A			A						A			H	C	A			C	A	V		C		C				A							
				30.5	4-7, 30-32	A	G						C	A	A	A			A						A			V	A	A				A	V				C				A							
				31.1	5-1, 30-32	A	G						C	A	A	A			A						A			V	A	A		F		A	V				A				A							
				32.6	5-2, 30-32	A	G						C	A	A	A			A						A	r		V	C	A		F		A	V				C				A							
				34.1	5-3, 30-32	A	G						F	A	A	A			A						A			V	C	A			C	A	V		C		A				A							
				35.6	5-4, 30-32	A	G						C	A	A	A			A						C			V	C	A			C	A	V		C		C				A							
				37.1	5-5, 30-32	A	G						R	A	C	A			C						F			V	C	A			A	A	V		C	F	C				A							
				38.6	5-6, 30-32	A	G						F	A	C	A			F		r				R			V	C	A			A	A	A		C		A				C							
				40.7	6-1, 30-32	A	G						F	A	C	A			F		r				R			V	C	C			C	A	A				C				A							
				42.2	6-2, 30-32	A	G						F	A	C	A			F		r				R			V	C	C			C	A	A		C		C				A							
				43.7	6-3, 30-32	A	G						C	A	C	A			C		r				C			V	A	A			A	A	V			F	C				A							
				45.2	6-4, 30-32	A	G						C	A	A	A	r		A		r				R			V	A	A			A	A	V			F	C				A							
				46.7	6-5, 30-32	A	G						C	A	A	A			A						R			V	F	C			C	A	V		C		C				A							
				48.2	6-6, 30-32	A	G						F	A	C	A			A		r							V	C	A			C	A	V		F		C				A							
				50.2	7-1, 30-32	B	B																					V	C	A			C	A	V		F		C				A							
				51.7	7-2, 30-32	A	G						R	A	A	A			A			r				r		V	F	F			R	A	V				C				A							
				53.2	7-3, 30-32	A	G						C	A	A	A			C									V		C			C	A	V		R		C				A							
				54.7	7-4, 30-32	A	G						C	A	C	A			F		r				R			V	C	A			C	A	V		F						A							
				56.2	7-5, 30-32	A	G						C	A	A	A			A									V	C	A			C	A	A								C							
				57.7	7-6, 30-32	A	G						C	A	A	A			A									V	F	C			R	V	V		R		C				A							
				59.7	8-1, 30-32	A	M						C	A	A	A			C									V	F	C			F	A	A		F						A							
				61.2	8-2, 30-32	A	M						C	A	C	A			C									A	F	F			F	A	V			R					A							
				62.7	8-3, 30-32	B	B																																											
				64.2	8-4, 30-32	A	P						F	A	A	A			F						F			V	C	C			C	A	A		R						C							
				65.7	8-5, 30-32	B	B																																											
				67.2	8-6, 30-32	B	B																																											
				68.5	8-7, 14-16	A	M						F	A	A	A			F			r						A	F	F			F	A	A								A							
				68.1	9-1, 30-32	A	G						C	A	A	A			C		f							V	A	C	C		C	A	V		F						A							
				69.6	9-2, 30-32	A	G						C	A	A	A			F		r							V	C	C		F	F	A	A								A							
				71.1	9-3, 30-32	A	G						C	A	C	A			C		f							A	C	C		F	F	A	A		R						A							
				72.6	9-4, 30-32	A	G						C	A	A	A			A		f							V	C	A		F	F	A	V								A							
			D. misconceptus (CN12c)	74.1	9-5, 30-32	A	G						F	A	A	A			A		A				R			V	C	A		C	C	A	A				F				A							
				75.6	9-6, 30-32	A	G						C	A	C	A			A		C							V	R	C		F	F	A	A				C				A							
				76.9	9-7, 12-14	A	G						C	A	A	A			A		A							V	C	C		R		A	A				C				A							
				77.6	10-1, 30-32	A	M						C	A	A	A			A		A							A	F	C		F	F	A	V				C				A							
				79.1	10-2, 30-32	A	M						F	C	C	A			C		F	f			R			A	F	F			R	A	V				F				F							

Pliocene	late	*D. brouweri* (CN12)	*D. misconceptus* (CN12c)	80.6	10-3, 30-32	A	M			F	A	C	A		C		A	r				f	A	F	C		C		V	V		F		C				A
				82.1	10-4, 30-32	A	M			R	C	C	C		C		C	f			R			F	F		F		A	A		F		F				F
			D. surculus (CN12b)	83.6	10-5, 30-32	A	M			F	A	A	A				F	C	R					C	C			F	A	A				F			r	
				85.1	11-1, 30-32	C	M			F	C	C	C		C		F		C		R			F	C		F		A	A								
				86.6	11-2, 30-32	A	P			F	C	A	A		A		C		A			C		F	C				A	V								
				88.1	11-3, 30-32	C	M				F	C	C		F	F	F		F		R	C		F	F		R		A	A								
				89.6	11-4, 30-32	A	M			C	A	C	A		A	C	C		C			C		C	C		F		V	V								
				—	11,CC	A	M			C	A	C		R	A	C	C		C			C		C	C		F		A	V								
				97.5	13-1, 30-32	A	M			C	A	C	C	R	A	C	A		A		F	C			C		C		A	A		F		C				
			D. tamalis (CN12a)	99.0	13-2, 30-32	A	M			C	A	C	C	F	A	C	A		A	A	F	C		C	A	F			A	H				C				
				—	13,CC	A	M			C	A	C	C	F	A	C	A		C	C	R	C		C	C		F		A	V				C				
				107.1	14-1, 30-32	A	M			C	A	A	A		A	F	A	r	C	A	R	C		C	A		F		A	V				C				
				108.6	14-2, 30-32	B	B																															
				110.1	14-3, 30-32	A	M			C	A	A	A		A	F	A		C	C	F	C		C	A		F		A	V				C				
				111.6	14-4, 30-32	A	M		r	A	A	A	A		A	C	V		C	A	F	A		C	A	A	A		V	V				A				
				113.1	14-5, 30-32	A	M			A	A	C	A		A	F	A		C	F	R	C		F	C	C	F		A	A				C				
				114.6	14-6, 30-32	C	M			C	C	C	C		C	C	A		C	C		F		C	C			F	A	A								
				116.1	14-7, 30-32	C	M			C	A	C	A		C		A		C	C		C		C	C		F	F	A	V			C					
				116.7	15-1, 30-32	C	P	F		C	A	A	A		F		F							C	A		C		A	V		A	A					
				118.2	15-2, 30-32	F	P								R				F																			
				119.7	15-3, 30-32	B	B																															
				121.2	15-4, 30-32	B	B																															
				122.7	15-5, 30-32	F	P				C	C	C		F	F	F		F										C	C								
				124.2	15-6, 30-32	C	P			C	A	C	A		A	C			C	C	F	A			C		C		A	A		C		C				
				125.7	15-7, 30-32	C	M			C	A	F	A		A	C			C	C	F	C		C	C			R	A	V				A				
				126.3	16-1, 30-32	A	M			C	A	C	A		A	C			C	C	R	A		A	F	C	F	C	A	V		C		C				
				127.8	16-2, 30-32	A	M			F	A	C	A		A	F			C	A	F	A		F	C		F	F	A	V				C	r			
				129.3	16-3, 30-32	A	M			C	A	A	A		C	F		r	C	C	F	C		F	C	F	C		A	V		C						
				130.8	16-4, 30-32	A	M			C	A	A	A		C	C			C	C	C	C		F	C		C	F	A	A		C						
				132.3	16-5, 30-32	A	M			C	A	A	A		A	C			A	C		A			F			F	A	V								
				133.8	16-6, 30-32	C	P				C	C	C		C	C	C		C			C			C				C	A								
				135.9	17-1, 30-32	C	M			C	C	A	A		A	C			F	C		C		F	C		F		A	V		C						
				137.4	17-2, 30-32	A	M			C	C	C	A		A	C			F	A	F	C			C		R		A	V				F				
				138.9	17-3, 30-32	A	M			C	C	C	A		A	C			F	C	F	C			C	F	F		A	A								
				140.4	17-4, 30-32	A	M			F	C	C	C		C	C	A		F	C	R	C		F	C		F		A	V								
				141.9	17-5, 30-32	A	M			C	C	A	A		A	C	A		F	A	F	C		C	C		F		A	V								
				143.4	17-6, 30-32	B	B																															
				—	17,CC	A	M			F	C	A	A		A	F	A		C	A	R	C		C	C	C	C		A	V		C		C				
				145.5	18-1, 30-32	A	M			F	A	A	A		A	C			C	A	F	C		F		F			A	V		F		F				
				147.0	18-2, 30-32	A	M			F	A	A	A		C	C	C		C	C		C		C	C	C			A	V		F		F				
				148.5	18-3, 30-32	A	M			F	A	A	A		C	C			C	C	F	C		C		F	F		A	V		F						
				150.0	18-4, 30-32	A	M			F	A	A	A		C	C			C	C	R	F		C	F	F	F		A	V								
				151.5	18-5, 30-32	A	M			C	A	C	A		A	F	C		C	A		C		F	F	F	F		A	V								
				153.0	18-6, 30-32	C	P				F	F	C		F	R	F					R		F					C	A								
				155.1	19-1, 30-32	C	M			F	A	A	A		A	F			C	C	F	C		C	C	C	F		A	V		F		F				
				156.6	19-2, 30-32	C	M			F	C	C	C		F	F	F			R		F		F	F	F			A	A								
				158.1	19-3, 30-32	F	P						C		F	F	F		F			F							F	A								
				159.6	19-4, 30-32	C	M			C	A	C	A		C	F			F	C	F	C		C	C	C			A	V								
				161.1	19-5, 30-32	C	M			F	C	C	C		C		F		F	C	F	C			C	F	F		A	A								
				162.6	19-6, 30-32	C	M			R	C	C	C		C	C	F		F			F		F	C	F			C	V								
				164.7	20-1, 30-32	A	M	R		C	A	C	A		A	F			C	C		C		C	A	F			A	V		F		C				
				166.2	20-2, 30-32	A	M			C	A	C	A		A	F			C	C		C		C	A	F			A	V		F		C				
				167.7	20-3, 30-32	B	B																															
				169.2	20-4, 30-32	C	M			F	C	C	A		F	R	C		C	F		C		P	C				A	V								
				170.7	20-5, 30-32	C	M			C	A	C	A		C	F	A		F	C		F		F	A	F			A	V				C				
				172.2	20-6, 30-32	B	B																															
				174.3	21-1, 30-32	C	M			C	A	A	A		C	F	A		F	C	F	F		F	C	C			A	V								
				175.8	21-2, 30-32	C	M			C	A	F	A		A	F	A		F	C		F		F	F	F			C	V								
				177.3	21-3, 30-32	C	M			F	A	C	A		C	F			F	C		F		F	C	F			C	V								
				178.8	21-4, 30-32	C	M			F	A	C	A	C	C	F			F	C		F		F	C	F			C	V								
				180.3	21-5, 30-32	C	M				C	C	C	C	C	F	C		F	C		F		F	F				F	A								
				181.8	21-6, 30-32	C	M			F	A	A	A	F	C	F	C		F	C	R	F		F	C	F	F		C	A			R					
				183.3	21-7, 30-32	C	M	F		F	C	A	C	A	A	C	A			C		C		C	F	F	F		C	V					r			
Pliocene	early	*R. pseudo-umbilica* (CN11)	*D. asymmetricus* (CN11b)	183.9	22-1, 30-32	C	M				A	C	F		C	F			F	F	F	F			C	F			A	V				F				
				185.4	22-2, 30-32	C	M			F	F	F	C	F	F	F			F	F		C			F	F			A	C								
				186.9	22-3, 30-32	C	M			F	C	C	C	F	C	C	F			C		F		F	F	F			A	V								
				188.4	22-4, 30-32	C	M			F	C	C	C	F	C	C	F		F	C		F		F	F	F			A	A								
				189.9	22-5, 30-32	C	M			F	A	C	C	C	C		C		F	F	F	F						F	A	A					C			
				193.5	23-1, 30-32	C	P			C	C	C	C	A	C		C		F	F		C		F	C			F	A	A					C	C		r
				195.0	23-2, 30-32	C	P			F	F	F	C	C	A	F	C		F	F	F	C			C		F		A	A					F	F		
				196.5	23-3, 30-32	A	M				C	C	C	C	C		C		F	F	F			F	F			F	A	A	C				F	F		C

Note: Abundance is characterized by V, very abundant; A, abundant; C, common; F, few; R, rare. For preservation, B, barren, P, poor; M, moderate; G, good. Lower-case letters indicate material considered to be reworked upsection or caved downhole. Under any taxon, cf denotes any similar but distinct form "compared with."

Table 1 (continued).

Age		Zone/Subzone		Sub-bottom depth (m)	Core-Section (interval in cm)	Relative abundance	Preservation	*Amaurolithus delicatus*	*A. primus*	*A. tricorniculatus*	*Braarudosphaera bigelowii*	*Ceratolithus acutus*	*C. cristatus/telesmus*	*Calcidiscus leptoporus*	*C. macintyrei*	*Coccolithus pelagicus*	*Discoaster asymmetricus*	*D. berggrenii*	*D. brouweri*	*D. intercalaris*	*D. misconceptus*	*D. quinqueramus*	*D. surculus*	*D. tamalis*	*D. triradiatus*	*D. variabilis*	*Discoaster* spp. (overgrown/dissolved)	*Gephyrocapsa* spp.	*Helicosphaera carteri*	*H. sellii*	*Pontosphaera japonica*	*P. multipora*	*Pontosphaera* sp.	*Pseudoemiliania lacunosa*	*Reticulofenestra haqii*	*R. pseudoumbilica*	*Rhabdosphaera* sp.	*Scyphosphaera* sp.	*Syracosphaera* sp.	*Sphenolithus abies*	*S. neoabies*	*Triquetrorhabdulus rugosus*	*Umbilicosphaera cricota*	Reworked species	*Discoaster deflandrei*	*D. loeblichi*	*D. multiradiatus*	*D. saipanensis*	*Isthmolithus recurvus*	Reworked Cretaceous (see text)
				198.0	23-4, 30–32	A	M						F	C	C	C	A		A	F	C		C	F	F	C			F	C	F	C		V	A	A				A	F		C							
				199.5	23-5, 30–32	C	M						F	C	F	C	C		A		F		C	F	C	C			F	F				A	A	A				F	F		C							
				201.0	23-6, 30–32	F	P							F					F	C	F		F	F	F					F			F	F	F	F				F	F		C							
				202.5	23-7, 30–32	C	P						F	C	C	C	A		A				C	C	F	C			F				F	A	A	A				F	F		C							
				203.1	24-1, 30–32	F	P							F			F		F										F	F		F		F	C															
				204.6	24-2, 30–32	C	M						C	A	A	A	A		A	C	C		C	F	F	C				F		F		A	V	A				C			C							
			D. asymmetricus (CN11b)	206.1	24-3, 30–32	C	M				F			C	A	A	A		A		C		C	F		C			C	C			C	A	V	A			R	C			A							
				207.6	24-4, 30–32	C	M						F	C	A	C	A		A		C		C	F					F					A	A	A				C	C		F							
				209.1	24-5, 30–32	F	P							F	F	F			F	F	F		F			F			F	F			F		C	F					F		C							
				210.6	24-6, 30–32	C	M						C	C	C	A	C		A	C	A		C	F		C			C	C			C	A	A	A				A	C		A							
				212.1	24-7, 30–32	C	M						F	A	C	A	C		C	C	C		A	F	F	C				C				A	A	A				C	F		C							
				212.7	25-1, 30–32	C	M						C	A	C	A	A		A		A		C	F	F	C			C	C		C		V	V	A				C	C		C							
				214.2	25-2, 30–32	C	M						F	A	C	C	A		A	F	A		C	F	F	C						F		A	V	A				A	A				r					
				215.7	25-3, 30–32	F	P						F	F	F	C	F				C					C				F					F	A					F									
				217.2	25-4, 30–32	C	M						C	A	F	A	C		A	F	A		C		F				C	C		F	R	C	A	A				C	C									
				218.7	25-5, 30–32	C	M						F	A	C	C	C		C	F	A		F			C			C	F		F		C	A	A				C	C									
				220.2	25-6, 30–32	C	M	F					C	C	F	C	C		A		A		C		F	F				C					A	A				C	C									
				221.7	25-7, 30–32	C	M						C	A	F	A	F		C	F	C		C		F	C			F	C	F	F		F	A	A				C	C		A							
				222.3	26-1, 30–32	C	P	C					F	C	C	C	F		C	F	A		C		R	C									A	A				F	C									
				223.8	26-2, 30–32	C	M	F						C	C	A	F		A	C	A		C			C			C	C		R			A	A				C	A									
				225.3	26-3, 30–32	C	M	F					F	C	C	C	R		C	C	A		C		C	F			F	C				A	A	A				C	A									
Pliocene	early	*R. pseudo-umbilica* (CN11)		226.8	26-4, 30–32	C	M						C	C	C	C	—		C	C	A		C		F	F				C				A	A	A				C	A									
				228.3	26-5, 30–32	C	M	F						A	F	A	F		C	F	A		C			C			C	C				A	A	A				C	A									
				229.8	26-6, 30–32	C	M						F	C	F	C	R		C	F	A		F			C			C	C	R	R		A	A	A				C	A		C							
				231.3	26-7, 30–32	C	M						F	C	C	C	F		C	R			C		F	C			C	C	F			C	A	A				C	A									
				231.9	27-1, 30–32	F	P							F	F				F	R			F		R	F				R				C	C	C				F	C									
				233.4	27-2, 30–32	F	P						R	C	C	C			C	F	A		C			C				F					C	A				F	C									
				234.9	27-3, 30–32	C	M						C	A	C	A	F		A	F	A		A			A			F	P				C	A	A				C	A									
				236.4	27-4, 30–32	F	P																												C	F					F									
			S. neoabies (CN11a)	237.9	27-5, 30–32	C	M	F					F	C	F	C	F		C	F	F		F		F	C			C	C					A	A				A	A									
				239.4	27-6, 30–32	C	M	R				r	F	A	C	A	F	r	F	F	C	r	F		R	A			C	C					A	A				A	A									
				240.9	27-7, 30–32	C	P						F	C	C	C	F		F	C	F		F		R	C			F	F		R			A	A				C	A									
				241.5	28-1, 30–32	A	M		F				F	A		A	F		A	C	A		C		F	A			F	F	R	R			A	A				A	A									
				243.0	28-2, 30–32	B	B																																											
				244.5	28-3, 30–32	C	M						F	A	F	A	R		C	A	A		F		F	A			F	C					A	A				C	A									
				246.0	28-4, 30–32	F	P							F																						F				F	F									
				247.5	28-5, 30–32	C	M					r	F	C		A			C	C	A		C		F	A			C	C				C	A	A				A	A									
				249.0	28-6, 30–32	F	P							F		F			C	C	F		C			C														C	C									
				—	28,CC	C	P						C	C	F	C	R		C	C	C		C			C				F	R				C	A				C	C									
				251.3	29-1, 30–32	F	P							F			R		F	F	F		F			C									C	C					C									
				252.8	29-2, 30–32	C	P						C	C	C	C			C	C	C		A		C	C			C	C					A	A		R		A	A						r			
				—	29,CC	C	M						C	C	F	A			C	F	C		F			F			F	F			F		A	A				C	A									
				260.7	30-1, 30–32	B	B																																											
				262.2	30-2, 30–32	R	P									F										R									F															
		A. tricorniculatus (CN10)	*C. rugosus* (CN10c)	—	30,CC	F	P	F	F	F				C		C			C	C	A		C			C									A	C				C	C									
				270.3	31-1, 30–32	B	B																																											

Pliocene	early	*A. tricorniculatus* (CN10)	*C. rugosus* (CN10c)	271.8	31-2, 30-32	B	B																																								
				273.3	31-3, 30-32	C	P	F		F				C		C			C	F	C		C			C				F					A	C				C	C						
				274.8	31-4, 30-32	C	M	F		F	F		F	C		C	R		C	C	C		C		F	C			F	F		R			A	A				C	C						
				276.3	31-5, 30-32	F	P	F					R	C	F	C			F		C		C			F				F					A	C				C	C						
				277.8	31-6, 30-32	F	P							F		C			F	F															C	C				F	F						
				—	31,CC	R	P							F																					F	R											
				279.9	32-1, 30-32	B	B																																								
				—	32,CC	F	P			R				C		C			C	C	C		C						F	F					F	C				C	C						
				289.5	33-1, 30-32	C	P	R	R	R		r		C	C	C	R		C	C	C		C			F				C					A	A				C	C						
				291.0	33-2, 30-32	R	P							R		F																				F											
				292.5	33-3, 30-32	C	P						R	F		C			C	C	C		C			A			F	F					A	F				C	C						
				294.0	33-4, 30-32	C	P	R	R					C	C	A			C	C	C		C			C			C	C					V	F				C	A						
				295.5	33-5, 30-32	C	P							C	F	F	R		F	F	C		C			F				C					A					F	C						
				297.0	33-6, 30-32	C	P	R	R					C		C			F	C	C		C		F	C				F					A	C				C	C						
				—	33,CC	B	B																																								
			C. acutus (CN10b)	300.1	34-1, 30-32	C	P	F				C		A	C	A	F		C	C	C		A			A									V	A				A	A						
			T. rugosus (CN10a)	—	34,CC	C	P	F	F					F	F	C	R		C	A	C		C			A			F	C					V	A				A	A	F					
				308.7	35-1, 30-32	C	P	F						C	F	C			F	C	C		C			C			C	C	R				A	A				A	A	F	F				
				310.2	35-2, 30-32	B	B																																								
				311.7	35-3, 30-32	C	P							C		C				C	C		C			C			F						A	C				C	C	F	F				
				313.2	35-4, 30-32	C	P							C					F	C	C		C			C			C	C					A	C				C	C	F	F				
				314.7	35-5, 30-32	C	P							F	F	C			F	F	C		F			F			F	F					A	C				F	F	F	R				
				316.2	35-6, 30-32	C	P							R		F			R				F			F									C	F											
				—	35,CC	F	P							R		F							F			F									C	F											
				318.3	36-1, 30-32	C	P							F	R	C			F	C	R		C			C			F						A	C				C	C		F				
				319.8	36-2, 30-32	C	P	R							F	C			C	C	R		A			A			F						C	C				A	A	F					
				321.3	36-3, 30-32	C	P							F	F	C			F	C	F	r	F			C				R	R				A	A				C	A	F					
				322.8	36-4, 30-32	F	P													R			R													F						R					
				324.3	36-5, 30-32	C	P							F									F			F									F	F				F							
Miocene	late	*D. quinqueramus* (CN9)	*A. primus* (CN9b)	325.8	36-6, 30-32	C	P								F	C			C		C	A	C			C				C			R		V	A				A	A		F				
				—	36,CC	C	P							F	F	C			C		C	C	C			C				C					V	A				A	A		F				
				327.9	37-1, 30-32	C	P		F					C	C				C	F	C	C	C			C				F					V	A				C	C	F					r
				329.4	37-2, 30-32	C	P	F	F					C	F	C			C	C	C	C				C				F					A	A	F						F				
				330.9	37-3, 30-32	B	B																																								
				332.4	37-4, 30-32	C	P							C	C	C			F	F		F	F			F			C	F			R		A	C	F			C	C	R	F				
				333.9	37-5, 30-32	C	P							F	F	F		R	C		F	C	R			F			F		R				V	C	F			C	C						
				335.4	37-6, 30-32	C	P							F	F	C			C	C	C	A	C			C				F					V	A				A	C						
				—	37,CC	C	P							F	F	C			C	C	C	A	C			C				F					V	A				A	C						
				337.5	38-1, 30-32	C	P							F		F		R	F		F	C	F			F									A	C				F	F						
				339.0	38-2, 30-32	C	P							C	F	C		F	C		C	C	C			C				F					A	C				A	C	F					
				340.5	38-3, 30-32	C	M	F			R			A	A	C			C		A	A	C			A				C					V	A				A	A	F	F				
				342.0	38-4, 30-32	B	B																																								
				343.5	38-5, 30-32	C	P	R	F					C	C	C		F	C	C	F	A	C			A				F					V	A				A	A	F					
				345.0	38-6, 30-32	C	P							A		A		F		F	C	A	C			A			C	C					V	A				A	A	C					
				—	38,CC	C	P	F						A	F	A		F	C	C		A								R					V	V				A	A	A					
				347.1	39-1, 30-32	C	P		F					C	C	C			F		F	C	C			C			C						A	A				A	A	F					
				348.6	39-2, 30-32	C	P		F					C	F	C			F	C	C	A	C			A									A	A				A	C	R					
				350.1	39-3, 30-32	C	P		F		R					F		C		F	F	A	C			V			F	R					A	A				C	C	C					
				351.6	39-4, 30-32	C	P		F					C		C		C	F			A				A			F	F					A	A				A	A	C					
				353.1	39-5, 30-32	C	P							F		C		F				C	F			C									A	C				C	C	F					
				354.6	39-6, 30-32	C	P		F					C								A	C			A	A																				
				—	39,CC	C	P							C		C		C	F		F	A	C			A			F	F					V	A				A	A	C					
				356.7	40-1, 30-32	C	P							F		F						F	F			F	F						R		C	C				C		F					
				358.2	40-2, 30-32	C	P							F		F		C				C	F			C	C		F						A	C				C	C	F					
				359.7	40-3, 30-32	C	P							C	F	C		C	F		R	C				A	A		F	F					A	C				A	A	F					
				361.2	40-4, 30-32	C	P	R								C		C				C				C	A								A	A				A	A				r		
				362.7	40-5, 30-32	C	P							F		C		C				C	F			C	A								A	A				A	C	F					
				364.2	40-6, 30-32	C	P							F		F		C				C				C	A			F					A	A				A	C	R					
				366.0	40,CC	C	P							C		C		C	F			C				C	A		F						A	A				A	A	F					

Table 2. Distribution of Miocene calcareous nannofossils, DSDP Hole 603 and Hole 603B.

Lithostratigraphic unit	Age	Zone	Subzone	Sub-bottom depth (m)	Core-Section, interval	Preservation	Relative abundance	*Amaurolithus delicatus*	*A. primus*	*Braarudosphaera bigelowii*	*Calcidiscus leptoporus*	*C. macintyrei*	*Catinaster calyculus*	*C. coalitus*	*Coccolithus pelagicus*	*Discoaster bellus*	*D. berggrenii*	*D. bollii*	*D. brouweri*	*D. calcaris*	*D.* sp. cf. *deflandrei*	*D. exilis*	*D. hamatus*	*D. intercalaris*	*D. kugleri*	*D. loeblichii*	*D. misconceptus*	*D. neohamatus*	*D. pentaradiatus*	*D. quinqueramus*	*D.* spp (overgrown/dissolved)	*D. surculus*	*D. variabilis*	*Helicosphaera carteri*	*H. sellii*	*Minylitha convallis*	*Pontosphaera* spp.	*Reticulofenestra haqii*/*R. gelidus*	*R. pseudoumbilica*	*Sphenolithus abies*	*S. moriformis*	*S. neoabies*	*Triquetrorhabdulus rugosus*	*Umbilicosphaera cricota*
					Hole 603																																							
IA	late Miocene	*D. quinqueramus* (CN9)	*A. primus* (CN9b)	363.2	16-1, 100–102	M	C				C	C			A				C								C			A		A	A	C	F			A	A	A			F	
				410.2	17,CC	M	C		R		C				C				C								C			C			A	C				A	C	C		C		
				412.0	18,CC	P	F								F		F										F						A							C				
				428.3	19-6, 100–102	M	A	R			A	C			A		F										F			C		F	A	C	C			A	A	C	C	A		C
				450.6	20-2, 50–52	P	C								F		F		F														C	F				A	F	A	C			
				462.2	21-3, 100–102	P	F	R							R		F		R											C	C							F	R					
IB			*D. berggrenii* (CN9a)	471.8	22-3, 100–102		B																																							
				507.2	23-1, 100–102	P	C					F			C		C		F							F	cf			C			A					A	C	F			R	
				524.3	24-6, 100–102	P	F								F		C										cf				C		C					F		R				
				548.6	25-3, 100–102	P	C			R	F	F			C		C	r	F							R	cf	R			C		C	C				C		F		F		
				558.2	26-3, 100–102	M	A								F		A		A								cf						C					F	F					
				563.8	27,CC		B																																					
				564.1	28-1, 7–8	P	F								F											F							C											
				578.5	29-4, 57	P	C										C		C	F				C			cf				C		C											
				584.9	30-2, 44–46	P	R													F											F		C											
				593.6	31-1, 102–104	P	F										C		F	F	R			F			cf			F	F		F											
		CN8	CN8b	604.9	32,CC	P	R																								R							F						
				617.3	33-4, 100–102	P	C				C	A			A				A					A					C				A			C	F	A	A	A	C		F	
				624.2	34-2, 132	M	VA				A	C			A				A					A				R	A				A	C		A	F		V	A	A	A	C	
				632.0	35-1, 109–111	M	VA				A	C			A	F			A	C				A				C	A				A	C	R	A	F	A	A	A	A			
		CN8	CN8a	641.6	36-1, 100–102	M	A				C	F			C			A	F					A				F	A				A	R				A	A	F		A	F	
				652.7	37-2, 100–102	P	A				F				F	F		A						C									A				R	V	A				F	
		CN7	CN7b	660.8	38-1, 100–102	P	C				F	R	F		F	F		C	F		R		F										C					C	C					
		C. coalitus (CN6)		672.0	39,CC	P	F							R		R		F						F									F					F	F					
	middle Miocene			686.0	40-4, 100–102	P	C					F		C	C	R								C			F						C	F				A	C	C		F		
				689.6	41-1, 105	M	A				C	F		C		F		F	F					C				C					A	F			F	V	A	C	F	F		
IC		*D. exilis* (CN5)	*D. kugleri* (CN5b)	704.5	42-5, 25	P	C					F			C			F	F														A					A	A	F				
				708.8	43-1, 100–102	P	C					C			C																		C	F				A	C					
				717.6	44-1, 25	P	R																	R									R											
				729.0	45-2, 47–48	P	F																								C		F					C	F					
				739.5	46-2, 140–143	P	C				C	C			F			C						C									C					A	A					
				747.8	47-2, 7–9	P	C								F										R								F					A	C					
				756.8	48-1, 104–105	P	F				F				F							C									C		C					C	F		F			
				766.4	49-1, 100–102	P	F					C			C							F			F								F	F				A	F		C			
				777.5	50-2, 100–102	P	F								F							R									C		F					F						
				785.0	51-1, 40	P	F				F				C									C	F								C					A	C		F			
				798.2	52-3, 100–102	P	C								F							C		C	F						A		C					A	F					
				804.9	53-1, 110–112	P	C				F				F							F		C	C													C	F			F		
				824.9	54-2, 42–44	P	C				F				C			C				F		C							C		F	F				A	C		F	R		
					Hole 603B																																							
IC	middle Miocene	CN5	CN5b	835.6	6M-4, 14	P	F ←*								F			R				F			F								C					C	C					
				869.4	7M,CC	P	F															F									F		F					F	F					
				870.9	8M-1, 146–147	P	C								A			F				F									C			F				A	C					
				892.6	9,CC		B																																					
				905.8	10,CC	P	C							c								C		C	R						C		C						F					
				908.8	11-2, 20	P	C								F										F						C		C					A	C					
		?	?	935.5	12-5, 100–102		B																																					
				940.9	13,CC		B																																					
ID	**			948.3	14-2, 64	P	EB								F																								F					
				960.4	15-4, 7	B	B																																					

Note: Abundance is characterized by V, very abundant; A, abundant; C, common; F, few; R, rare; B, barren; EB, essentially barren. For preservation, P, poor; M, moderate; G, good. Lower-case letters indicate material considered to be reworked upsection or caved downhole. Under any taxon, cf denotes any similar but distinct form "compared with." * indicates Sample 603B-6,CC (834.8 m): quartz sand turbidite with upper Eocene nannofossils. ** indicates early-middle Miocene based on radiolarians and fish teeth (Hart and Mountain, this volume).

long washed interval above, this LO could be as high as 333.1 m, which would be close to its level in Hole 603C.

Samples 603-16-1, 100–102 cm through 603-21-3, 100–102 cm (Table 2) are assigned to the *A. primus* Subzone (CN9b), based on the interval from the datums discussed above down to the first occurrence of *A. delicatus.*

The *D. berggrenii* Subzone (CN9a) is present from Samples 603-22-6, 100–102 cm to 603-31-1, 102–104 cm, based on the common *D. berggrenii* in the latter sample. Nannofossils in this interval are generally poorly to moderately preserved, and their numbers are few to abundant. In Core 603-31, *D. berggrenii* and associated forms comprise an interesting plexus in which various degrees of birefringence may be noted among the specimens. Some forms with suppressed central area knobs would be classified as *D. misconceptus* (Theodoridis) if bifurcations were present at the ray terminations, but none have been observed in these samples. In Table 2, such specimens are denoted by "cf." under *D. misconceptus.* The absence of ray bifurcations could be due to the poor preservation in this part of the section. Alternatively, these may be forms ancestral to *D. misconceptus.*

The interval between Samples 603-26-3, 100–102 cm and 603-33-4, 100–102 cm contains rather sparse assemblages characterized by a few large discoasters and a near absence of placoliths. Sample 603-27,CC is barren.

From Samples 603-32,CC through 603-35-1, 109–111 cm, the assemblages are moderately preserved and nannofossil abundances in selected samples are relatively high, as shown in Table 2. Abundances in samples adjacent to those plotted, however, may be quite low, with coccoliths absent or present in only trace amounts. Nevertheless, abundances of selected samples in this short interval are the highest abundances found between Section 603-16-1 and the base of the hole. The top of this interval of relatively high abundance may be marked by a slight hiatus, but if so, the time value of such a break is relatively insignificant.

In Sample 603-34-2, 132 cm, *D. pentaradiatus* clearly do not exhibit the optical birefringence of the younger *D. misconceptus* (see Theodoridis, 1984). The distinction between broken-tipped *D. pentaradiatus, D. bellus,* or *D. quinqueramus* can be difficult to make, but we see no evidence of the latter two species in these samples. It is also interesting to note that about 15% of the *D. variabilis* in this sample are 5-rayed.

Based on the absence of both *D. berggrenii* and *D. bollii*, as well as the presence of the nonbirefringent *D. pentaradiatus* (= *D. prepentaradiatus* of Bukry), we assign the interval from Samples 603-33-4, 100–102 cm to 603-35-1, 109–111 cm to the *D. neorectus* Subzone (CN8b) of the *D. neohamatus* Zone. *Minylitha convallis* is abundant in this interval, and may be more widely distributed than shown on the range chart (Table 2).

Extending from Samples 603-36-1, 100–102 cm to 603-37-2, 100–102 cm is the *D. bellus* Subzone (CN8a) of the *D. neohamatus* Zone. Preservation in this interval is moderate to poor and nannofossils are relatively abundant. We use the LO of *D. bollii*, a secondary marker, to denote the top of the subzone. Abundant throughout this short interval, it disappears abruptly at the top of the subzone, perhaps indicating another erosional disconformity.

The *Catinaster calyculus* Subzone (CN7b) of the *D. hamatus* Zone can be distinguished in this hole in only one sample, 603-38-1, 100–102 cm. Preservation in this sample is poor, but nannofossils are common. This is the only sample from Site 603 in which *D. hamatus* and *C. calyculus* are present. Rare specimens of the latter are well preserved (Pl. 1, Figs. 8–11), but the few *D. hamatus* noted are broken. It is possible that all of this material has been reworked. The restriction of this zone to a relatively short interval of section and the absence of Subzone 7a (in which *C. calyculus* would be absent) indicate a significant hiatus at this point in the section (see discussion below under "Sedimentation Rates and Correlations with Seismic Reflectors").

The *C. coalitus* Zone (CN6) is present from Samples 603-39,CC through 603-41-1, 105 cm. Preservation in this interval ranges from poor to moderate. Nannofossils are relatively sparse at the top of this interval in Sample 603-39,CC but are surprisingly abundant at the base of this zone in Sample 603-41-1, 105 cm.

The *D. kugleri* Subzone (CN5b) extends from Sample 603-42-5, 25 cm to the bottom of the hole (Core 54). Thus Hole 603 is tentatively assigned a maximum age of middle Miocene by nannofossils. The basal sample yielded an anomalously young assemblage (not shown in Table 2). Small chunks recovered in Sample 603-54,CC were interpreted as cavings from above, because they contain nannofossils such as *D. quinqueramus*, which represents a much younger assemblage. Nannofossil preservation is generally poor in this interval; many of the six-rayed discoasters in these samples cannot be identified because they are too broken, dissolved, or overgrown. Nannofossils are generally common to few in abundance. One sample (603-44-1, 25 cm) contains only the rare occurrence of two species of discoasters.

It is interesting to note that *D. kugleri* in Sample 603-51-1, 40 cm exhibits terminal bifurcations of the rays. Such a morphology was not documented by Martini and Bramlette (1963) in their original description. However, we note in Plate 1, Figures 1–4 that this variation is present in the topotype material from Trinidad (Sample BO 355).

Hole 603B (Table 2)

Hole 603B (35°29.71′N; 70°01.71′W; water depth 4633 m) was located 30 m west of Hole 603. The calcareous nannofossils in the top four cores from Hole 603B do not provide stratigraphically significant information because these are from wash cores taken over approximately 831 m of section. Nevertheless, Sample 603B-1M is assigned to the *Discoaster brouweri* Zone (CN12); Samples 603B-2M through -4M are assigned to the *D. quinqueramus* Zone (CN9). This same 831 m of section was cored in Holes 603 (Cores 1 through 51) and 603C, which offer a more precise biostratigraphy.

Core 603B-5 (821 to 831 m sub-bottom) is equivalent in age to Core 603-52 (*D. kugleri* Subzone, CN5b). Common *D. kugleri, D. variabilis, D. intercalaris, D. exilis*, and *D. deflandrei*, as well as a few *Helicosphaera carteri* and *Calcidiscus leptoporus*, occur within this interval.

Wash Cores 603B-6M through 8M represent approximately 60 m of cored sediment (831–892 m sub-bottom). As indicated in Table 2, these sediments contain a middle Miocene assemblage (CN5b) represented by relatively common *D. exilis*, few *D. deflandrei, D. kugleri*, and *Reticulofenestra pseudoumbilica*, and rare *Helicosphaera burkei* in Section 603B-8-1.

A thin turbidite layer in Core 603B-6M,CC contains a diverse and well-preserved nannofossil assemblage of late Eocene age mixed with smaller numbers of middle Miocene coccoliths of Zone CN5. Although not plotted on the range chart (Table 2), the Eocene coccoliths and their abundances are as follows: *D. tani nodifer* (R), *D. saipanensis* (F), *D. barbadiensis* (F), *R. bisecta* (A), *R. umbilica* (C), *R. reticulata* (C), *R. daviesii* (C), *Coccolithus formosus* (C), *C. pelagicus* (C), *C. eopelagicus* (C), *Chiasmolithus oamaruensis* (F), *Zygrhablithus bijugatus* (C), *Sphenolithus* spp. (C), *Neococcolithes dubius* (R), *Helicosphaera seminulum* (R), *Pontosphaera pulcheroides* (F), and *P. multipora* (R). The presence of *N. dubius* and the absence of *Isthmolithus recurvus* place this assemblage in Subzone CP15a. The significance of this allochthonous assemblage is discussed below under "Eocene Coccoliths in the Middle Miocene Turbidite of Core 603B-6M".

Sample 603B-10,CC contains common *D. exilis, D. intercalaris, D. variabilis*, and rare *D. kugleri*. With the exception of a few *R. pseudoumbilica*, placoliths are not present. The sample also contains common catinasters. We consider this occurrence anomalous: it is 216 m below the last recorded *Catinaster* (which were consistently present over a 21.5 m section higher in the hole). The simplest explanation is that Sample 603B-10,CC may be contaminated by cavings from farther up the hole.

Core 603B-11M was cored over a 20-m interval. The occurrence of *D. kugleri, D. exilis, R. pseudoumbilica*, and *Calcidiscus macintyrei* assigns this core to the *D. kugleri* Subzone (CN5b), the same as Core 603B-10. *Cyclicargolithus floridanus* is not present.

Unidentifiable discoasters are present only in Section 4 of Core 603B-12. The rest of Core 12 is barren, as is all of Core 603B-13.

Core 603B-14 is barren except for Section 2, which contains few to rare *D. exilis, D. bellus, D. braarudii, D. intercalaris, R. pseudoumbilica*, and pristine *Calcidiscus leptoporus*. These apparently represent downhole contaminants, since a mixture of Pleistocene through middle Miocene specimens seems to be present. Also present are overgrown specimens similar to *D. woodringii* and variants which may represent *in situ* coccoliths.

In summary, no Tertiary nannofossil assemblages below Core 503B-11M are considered stratigraphically significant. The oldest autochthonous assemblage that can be dated with confidence, Core 603B-11M, is assigned to the *Discoaster kugleri* Subzone (middle Miocene).

HOLE 603C: CORRELATIONS WITH MAGNETOSTRATIGRAPHY

Pliocene/Pleistocene Boundary

The magnetostratigraphy from Hole 603C (Canninga et al., this volume), Pliocene and early Pleistocene nannofossil age datums applied by Backman and Shackleton (1983), and the FO or LO datums of the Pliocene and early Pleistocene nannofossil markers from Hole 603C are correlated and discussed in this section.

The Pliocene/Pleistocene boundary is marked by the LO of *Discoaster brouweri* which, according to Backman and Shackleton, (1983) was approximately 1.88 Ma. This datum occurs at a depth of 29 m at Site 603. Interestingly, the oldest part of the Olduvai Subchron occurring at 1.87 Ma (Lowrie and Alvarez, 1981) is at a depth of approximately 44 m in Hole 603C. It is possible that *D. brouweri* has been reworked upsection, thus accounting for this 15-m stratigraphic discrepancy, but that is unlikely. The reason is that just prior to the LO of *D. brouweri* in Sample 603C-4-6, 30–32 cm, *D. triradiatus* is very prolific, comprising 20–40% of the discoasters in Samples 603C-4-6, 30–32 cm through 603C-5-3, 30–32 cm. According to Backman and Shackleton (1983) and as observed elsewhere (Parker et al., 1985), the final 0.15 Ma of the range of *D. brouweri* is characterized by a high proportion (20%) of *D. triradiatus*. Both *D. brouweri* and *D. triradiatus* have synchronous extinctions. Could both of these species have been systematically reworked? We think not, which leads us to believe that at least at Site 603, the LO of *D. brouweri* occurs at a somewhat later date than the date of 1.88 Ma suggested by Backman and Shackleton (1983), assuming, of course, that the magnetics are in order from Hole 603C.

Alternatively, with a sedimentation rate of 10.1 cm/10^3 yr. at Site 603 (Canninga et al., this volume), the ± 0.1 Ma accuracy of the nannofossil age datums of Backman and Shackleton (1983) would indicate a maximum discrepancy of ± 10 m between magnetic datums and the last occurrences of the nannofossil zonal markers at Site 603. This might account for at least a portion of the 15-m difference discussed above. Our sampling intervals might account for up to another 1.5 m.

Pliocene

The LO of *Discoaster misconceptus* (= *D. pentaradiatus*) lies at 74.1 m sub-bottom in Hole 603C. The extinction of *D. misconceptus* is dated at 2.35 Ma by Backman and Shackleton (1983). The top of the Gauss Chron is dated at 2.40 Ma by Lowrie and Alvarez (1981) and is located at a depth of approximately 81 m in Hole 603C (Canninga et al., this volume). The LO of *D. surculus*, dated by Backman and Shackleton (1983) at 2.41 Ma, is located at a depth of 79.1 m in Hole 603C. These two biohorizons closely correlate with the top of the Gauss Chron and fall well within the uncertainty ± 0.1 Ma of the age assignments given the extinctions of *D. surculus* and *D. misconceptus* by Backman and Shackleton (1983). Furthermore, there appear to be no noticeably reworked specimens in this interval.

The LO of the *Sphenolithus* spp. occurs at 183.9 m sub-bottom in Hole 603C. The extinction of *Sphenolithus* spp. is dated by Backman and Shackleton at 3.45 Ma. The top of the Gilbert Chron is dated at 3.40 Ma (Lowrie and Alvarez, 1981) and occurs at a depth of approximately 175 m in Hole 603C (Canninga et al., this volume). The close correlation between the magnetic datum and the *Sphenolithus* spp. datum is well within the uncertainty, as discussed earlier, of the age assignments given the LO of the *Sphenolithus* spp. and the paleomagnetic age for the top of the Gilbert Chron.

Figure 5 further illustrates the close correlation between selected early Pleistocene and Pliocene nannofossil datum age dates, the depth of these datums at Site 603, the magnetic polarity scale of Lowrie and Alvarez (1981), and the magnetic polarity stratigraphy of Hole 603C (Canninga et al.; Moullade; both this volume). Because core recovery was extremely poor in Cores 603C-30 through -34, it is not realistic to attempt to correlate the extinction of *Amaurolithus* spp. or the first occurrence of *Ceratolithus rugosus* with the established magnetics.

Miocene/Pliocene Boundary

For Hole 603C, we pick the Miocene/Pliocene boundary on the LO of the nannofossil *Discoaster quinqueramus*, which occurs at 325 m. Using planktonic foramini-

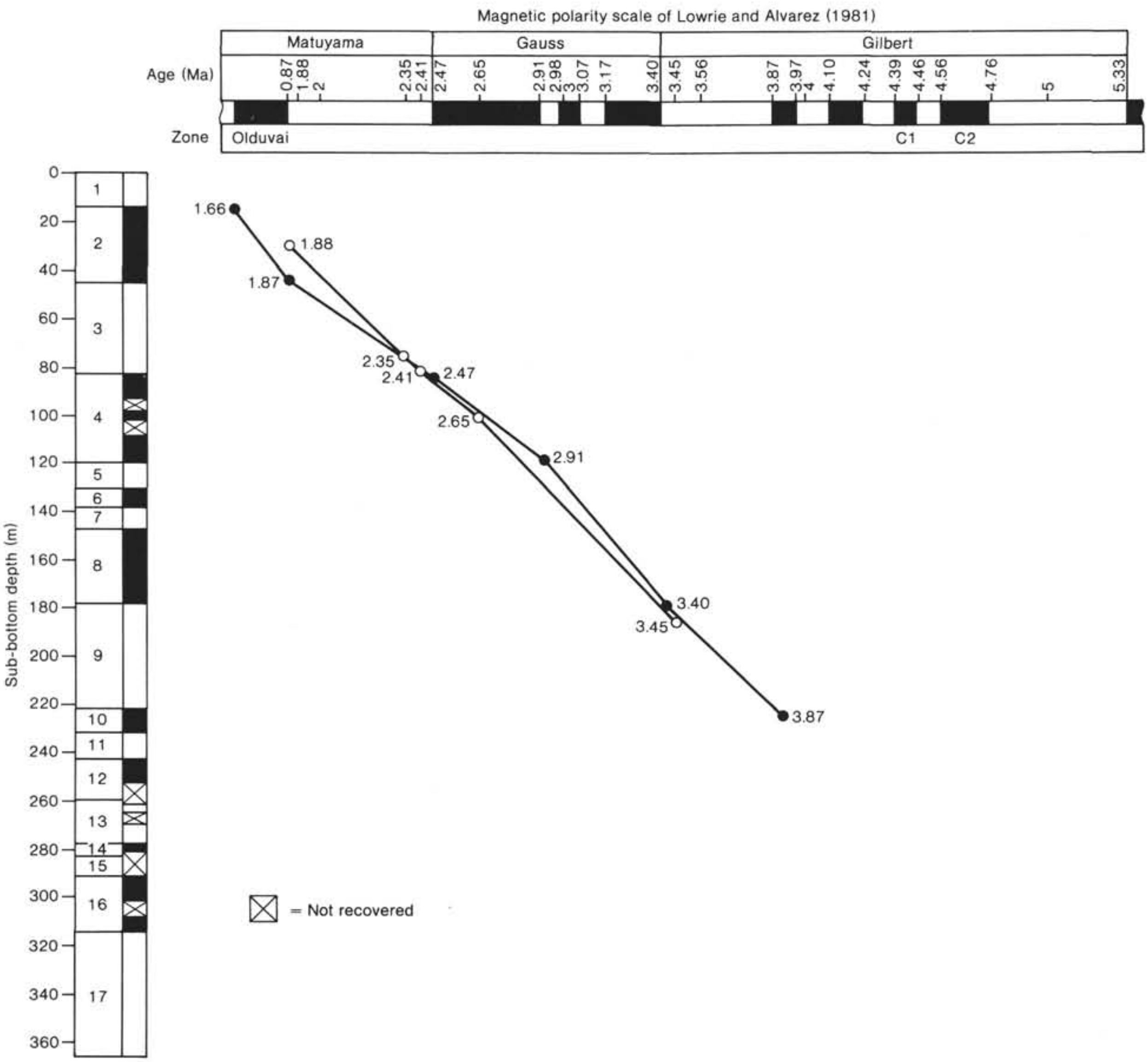

Figure 5. Correlation between calcareous nannofossil datums for Hole 603C and paleomagnetic stratigraphic scales. Vertical scale is the paleomagnetic polarity record from Hole 603C (Canninga et al., this volume). Horizontal scale is the Standard Polarity Time Scale of Lowrie and Alvarez (1981) against which are plotted the nannofossil age datums of Backman and Shackleton (1983). Dots represent points of correlation between the paleomagnetic record of Hole 603C and the Standard Polarity Time Scale of Lowrie and Alvarez (1981). Open circles represent points of correlation between select nannofossil age datums of zonal markers (Backman and Shackleton, 1983) and the sub-bottom depths of these nannofossil datums in Hole 603C. A strong linear correlation between lines connecting these two sets of points seems to indicate that zonal markers were not reworked in this part of the section and supports the work of Backman and Shackleton (1983) for the western North Atlantic province.

fers in nearby Hole 603, Moullade (in Ma'alouleh and Moullade; Site 603 chapter; both this volume) places this boundary at a sub-bottom depth of not less than 420 m, which is at least 50 m deeper than the bottom of Hole 603C at this site. The paleomagnetic Miocene/Pliocene boundary is inferred by Canninga et al. (this volume) to be also somewhere below the total depth of Hole 603C. They assign the lower 44 m of the hole (their magnetozone 17) to the reversed interval below the C2 Subchron at the base of the Gilbert Chron. We believe all three of these observations are correct, and that the differences are merely due to different practices currently used by specialists to place the "nannofossil," "planktonic foraminiferal," and "paleomagnetic" Miocene/Pliocene boundaries. As there seems to be at present no consensus among specialists or a universally agreed-upon scheme for defining the Miocene/Pliocene boundary, the placement of this boundary at Site 603 bears some discussion. The greatly expanded and apparently continuous nature of the section at this locality also makes our observations pertinent to the larger question of how to correlate placement of the boundary by the three unrelated disciplines mentioned above.

As just stated we believe that the datums and correlations as given above are correct. From the data, the succession of events at Site 603 is as follows:

"Nannofossil Miocene/Pliocene boundary": 325 m (within the Gilbert Chron, below Subchron C2)

"Magnetostratigraphic Miocene/Pliocene boundary": somewhere below 360 m

"Planktonic foraminifer Miocene/Pliocene boundary": 420 m

We believe that this is the correct order of events for the criteria used, and that had it been possible to identify the base of the Gilbert Chron in the sequence, it would fall between the nannofossil and planktonic foraminiferal datums used. Just which of these events should be taken as the "true" Miocene/Pliocene boundary is, at present, essentially a matter of preference in correlating these datums into the appropriate stratotypes. We do not state a strong preference here, but we do wish to give the range of current opinion on that as well as on the paleontologic criteria used.

Nannofossil Criteria

Following Gartner et al. (1984) and Haq (1984), we accept rather arbitrarily the extinction of *Discoaster quinqueramus* as the nannofossil datum to mark (approximate) the Miocene/Pliocene boundary. Both Bukry (1973) and Martini (1971), however, place this datum below the boundary. Martini (1971) suggests no datum to mark the boundary, and Bukry (1973) tentatively suggests the top of the overlying *Triquetrorhabdulus rugosus* Subzone, which is marked by the FOD of *Ceratolithus acutus* and the LAD of *T. rugosus*. We recognized both of these latter datums in Core 603C-34, which, according to Canninga et al. (this volume), fall within Subchron C2 of the Gilbert Chron. We thus could delimit all of Bukry's subzones in the vicinity of the boundary and could distinguish his datums in the order he suggested. Gartner et al. (1984, p. 30), on the other hand, state that the appearance of *C. acutus* and the extinction of *D. quinqueramus* "coincide in some ideal sections," therefore they use these combined datums to delimit their "nannofossil" Miocene/Pliocene boundary.

As to correlation of the extinction of *D. quinqueramus* with magnetic stratigraphy, there is an equal range of opinion. Berggren et al. (in press) place it within the reversed interval in mid Chron 5 (between events a and b), well within the upper Miocene by most definitions. Gartner et al., (1984), however, place it within the lower Gilbert chron, about halfway between the base of the Thvera event and the Gilbert/Chron 5 boundary.

Based on our results from Site 603, therefore, we affirm Bukry's (1973) succession of nannofossil zones and datums, but, as did Gartner et al. (1984), we choose the extinction of *D. quinqueramus* as the nannofossil datum that best approximates the Miocene/Pliocene boundary. Similarly, we find that datum to fall between the Thvera Event and the Gilbert/Chron 5 boundary (but closer to the former than the latter, rather than halfway between as indicated by Gartner et al., 1984). On the other hand, we do not find that the LO of *D. quinqueramus* coincides with the FO of *C. acutus*, but rather that this latter datum and the LO of *T. rugosus* fall higher in the section, within Gilbert Subchron C2. One could argue from this that all of our last occurrence datums could indicate reworking upsection. Reworking might be expected among the antidunal contourite deposits in this portion of the section which underlies the Hatteras Outer Ridge, but this is not supported by the apparently correct succession of first occurrence datums in the sequence. Furthermore, the amauroliths and triquetrorhabdids in this part of the section are relatively scarce and delicate; thus it seems unlikely that they would survive redeposition in numbers sufficient to allow their detection in our smear slides.

Planktonic Foraminiferal Criteria

As stated previously, the "foraminiferal Miocene/Pliocene boundary" was not reached in Hole 603C, but was picked at approximately 420 m sub-bottom depth in Hole 603, where the FO of *Globorotalia margaritae*, the presence of *G. juanai*, and specimens evolutionarily intermediate between these two species have been noted (Site 603 chapter; Ma'alouleh and Moullade; both this volume). The evolutionary transition between the two species has been dated at or very close to the Miocene/Pliocene boundary by Kennett and Srinivasan (1983), and is taken as evidence to mark the boundary at Site 603.

Although opinions among specialists differ, Berggren, Kent, Flynn, et al. (1985) and Berggren, Kent, and Van Couvering (1985) correlate the FO of *G. margaritae* to mid Chron 5 between events a and b. They note, however, that in the literature, the FO of *G. margaritae* is "usually recorded at or slightly above a level thought (by indirect correlation) to lie in the basal Gilbert chron" (Berggren, Kent, and Van Couvering, 1985), appendix II, table 6). Berggren and his colleagues instead link the Miocene/Pliocene boundary via the LO of *Globoquadrina dehiscens* and the FO of *Globorotalia tumida* with the base of the Gilbert Chron.

Based on the comparatively low level in the section at which the FO of *G. margaritae* is encountered at Site 603 (at least 95 m below the LO of *D. quinqueramus*), we would agree with Berggren and his colleagues' correlation of this foraminifer datum with the magnetic time scale. We note, however, that they also correlate the extinction of *D. quinqueramus* to the same level (mid Chron 6), a correlation which is clearly not supported by the succession at Site 603, where the two datums are widely separated.

Summary and Conclusion

The nannofossil and planktonic foraminiferal datums used to pick the Miocene/Pliocene boundary in the expanded section at Site 603 are separated by 95 m of section. The Gilbert/Chron 5 boundary probably lies between these two microfossil datums. All three of these levels have been linked to the Miocene/Pliocene boundary. At this site, the nannofossil datum closest to the boundary seems to be the LO of *Discoaster quinqueramus*, in that the LO of *Triquetrorhabdulus rugosus* and the FO of *Ceratolithus acutus* occur in Gilbert Subchron C2.

EOCENE COCCOLITHS IN THE MIDDLE MIOCENE TURBIDITE OF CORE 603B-6M

The occurrence of abundant upper Eocene nannofossils in the glauconite- and quartz-rich, silty sand turbidite layer recovered in the core catcher of Core 603B-6M is significant. These coccoliths are rather well preserved and were probably eroded from an Eocene carbonate outcrop along the slope of the continental margin. Such outcrops are known today off the eastern seaboard, and one of the more extensive has been mapped in part off New Jersey in the vicinity of DSDP Sites 604 and 605 (Robb et al., 1981, 1982). Core 603B-6M provides evidence of the exposure of such an outcrop during CN5b time (13.1 to 10.8 Ma, according to Berggren, Kent, Flynn, et al., 1985), and could possibly signal the initiation of canyon cutting along the slope during this interval.

SEDIMENTATION RATES AND CORRELATIONS WITH SEISMIC REFLECTORS

Coccoliths are sufficiently abundant in the Neogene sediment drift sequence at Site 603 to allow calculations of sedimentation rates by these fossils alone, and to suggest correlations (or lack thereof) of major seismic reflection horizons and oceanographic events with hiatuses. The major reflection horizons are outlined in Figures 2 and 3 and are discussed in the Site 603 chapter and in a modeling study by Biart (this volume). As noted in Figure 2, a well-defined set of sediment waves is developed above reflection Horizon X, beginning just below Horizon M_2. A sharp erosional disconformity is indicated within the sediment wave sequence by Horizon M_2, which truncates underlying reflectors as shown in the partial profile in Figure 3. Other less prominent reflection horizons are labeled in Figure 3 within the drift deposits, and a series of fine but evenly spaced reflectors characterize the sediment wave sequence above M_2.

Our data are summarized in Figure 6. The upper portion of the curve down through the LOD of *Amaurolithus primus* is based on absolute dates (for the events indicated) given in Backman and Shackleton (1983). A 5-Ma date for the LOD of *Discoaster quinqueramus* is estimated from the results of the present study. Dates for all datums and zones below this point on the curve are from Berggren, Kent, Flynn, et al. (1985).

The curve above 600 m (within the sediment wave sequence) is remarkably uniform, with an average sedimentation rate of 87 m/Ma. Rates just below 600 m, through nannofossil Subzone CN8b, are over twice as great at 192 m/Ma. Although carbonate accumulation was maximum for the hole through this interval, the higher sedimentation rate must indicate some other process at work, such as rapid accumulation during the latter stage of late Miocene canyon cutting higher on the continental margin (see discussion below under "Correlation of Reflection Horizon Merlin/M2"). We assume that the same processes were at work during CN8a and CN7 time, but that the section has been removed by erosion. We postulate, therefore, the same high sedimentation rate for the interval bounded by the hiatuses shown in Figure 6. The curve through this interval, of course, is uncertain because of the disconformities present and is constrained only by the error boxes provided by the zones sampled. The sedimentation rate through Subzones CN8a and CN7b, therefore, could be less than indicated.

The sedimentation rate indicated by the curve through box CN5b cannot be less than shown because of the limiting datums, but the rate could be greater if the FOD of *Discoaster kugleri* was not actually reached at 911.5 m, the point at which nannofossils essentially disappear from the section through dissolution below the calcite compensation depth. Our placement of the FOD of *D. kugleri* there is quite arbitrary, but not unreasonable in that it generates a sedimentation rate curve consistent with the one which is well documented above 630 m. Within the lowermost portion of the Miocene section (below 911.5), sedimentation rates must have fallen off considerably at some point. From their study of fish teeth, Hart and Mountain (this volume) date lithostratigraphic Subunit ID close to the early/middle Miocene boundary, suggesting that it could well be early Miocene in age. Taking the early/middle Miocene boundary as an approximation for the base of lithostratigraphic Unit I, the sedimentation rate for the Miocene section below 911.5 m would only be 15.3 m/Ma. Thus we consider the curve through Zones CN6 and CN5b reasonable though somewhat tenuous. We see no reason why the rate should be any higher than shown, and simply note that it cannot be any lower because of the ages assigned the datums which define the zone.

While Site 603 was being drilled, sedimentologists were alert for sandy contourite laminae which would explain the fine, uniform pattern of reflections within the sediment wave sequence. None were found. The entire upper sequence consists of muddy contourites with no appreciable sands encountered within the first 800 m. Likewise, the paleontologists were alert for any hiatuses which might indicate disconformities that could be correlated

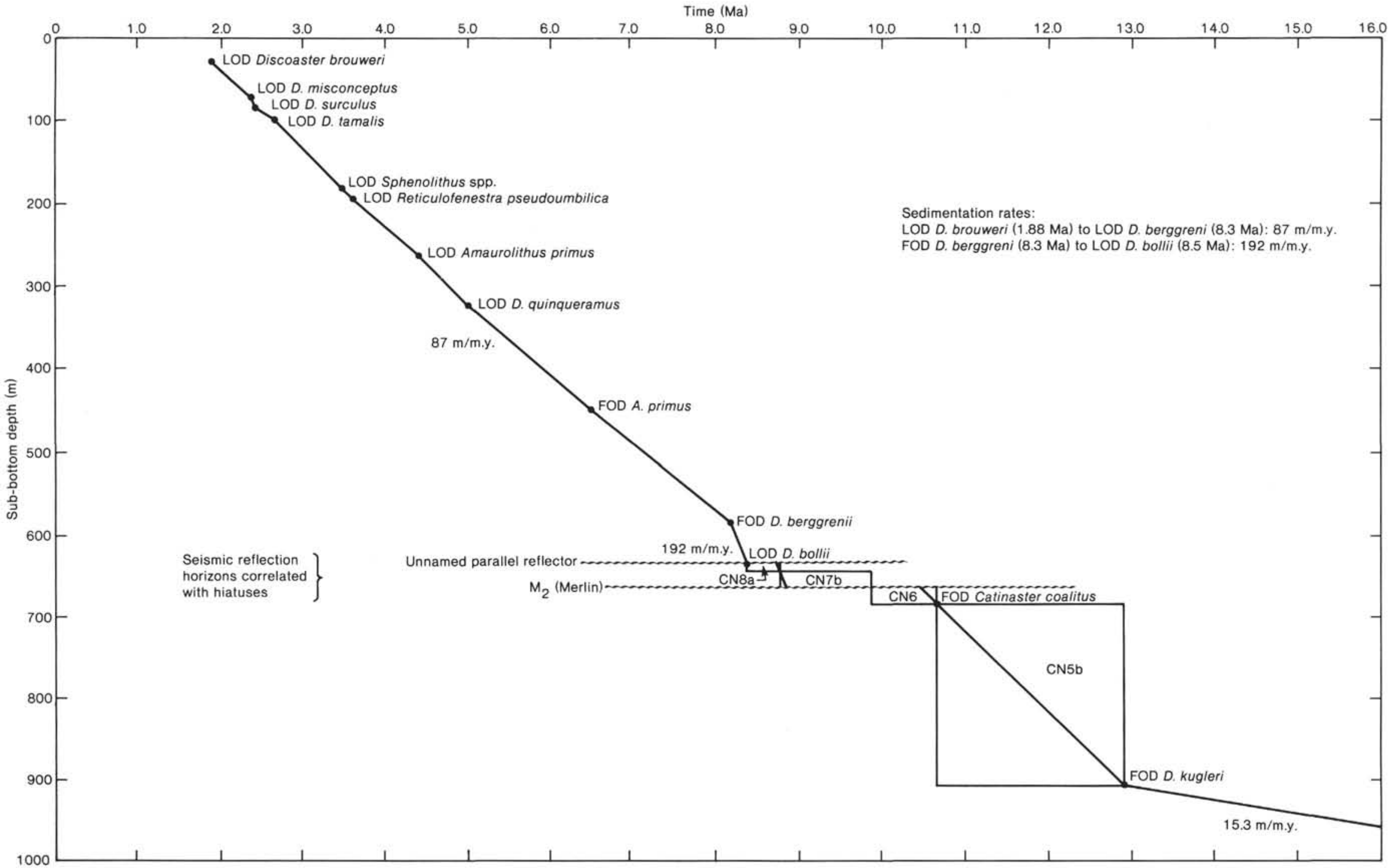

Figure 6. Sedimentation rates, hiatuses, and correlated reflectors for the Neogene sediment drift drilled at Site 603.

with seismic reflectors. As indicated in Figure 6, no such disconformities could be discerned by nannofossils within the first 600 m of section. Instead, all nannofossil zones are accounted for, and the sedimentation rate is remarkably uniform at about 87 m/Ma. Planktonic foraminifers in the Plio-Pleistocene section of Hole 603C have also been studied in some detail, and no hiatuses have been recorded or suspected (Ma'alouleh and Moullade, this volume; see also Site 603 chapter).

A possible hiatus may be indicated at about 600 m (just below Cores 603-31 or -32) by a change in the abundance of nannofossils in selected samples beginning in Core 33. This, however, is not a well-dated portion of the section since Core 32 is essentially barren and we cannot document missing section. Identification of a hiatus between 632 and 642 m (between Cores 35 and 36) is also somewhat tentative, in that no complete zone or subzone is missing. This hiatus is based on the rather abrupt disappearance of *Discoaster bollii*, which had been abundant in previous cores. The interval for Subzone CN8a is also quite short, compared to that for CN8b.

Better documented is the hiatus which separates Zones CN7 and CN6. There, we are unable to detect Subzone CN7a, and Subzone CN7b is restricted to only one sample in which the few *D. hamatus* present are broken. This clearly represents a significant disconformity, above which the CN7 material observed may even be reworked. Zone CN6 is also quite short (about 20 m), and appears to have been truncated by the disconformity. In contrast to Zones CN8a to CN6, which taken together might be considered a "condensed" interval perhaps cut by several hiatuses, Subzone CN5b is well represented by at least 200 m of section deposited at a rate interpreted to be equivalent to that of the upper portion of the section.

Coccoliths within Subzone CN5b are generally sparse and poorly preserved; thus it is doubtful if hiatuses could be detected within this long interval. Horizon X has been traced along multichannel seismic line 77 (Fig. 2) by Tucholke and Laine (1983) and Mountain and Tucholke (1985), who interpret it as a time-transgressive seismic facies boundary (not a time marker), which overlies the hummocky and shingled reflectors that generally comprise the lower portion of the post-Horizon A^u sedimentary section along the continental rise. At Site 603, it has been picked variously at about 740 m within CP5 (Fig. 2; see also Site 603 chapter) or at the CN5b/CN6 boundary in the modeling study by Biart (this volume). There it would also coincide with the top of lithostratigraphic Subunit IC, the point at which biogenic silica increases and carbonate decreases down the section.

The next reflection horizon up the column from Horizon X, Horizon M_2, is also the most prominent within the sediment drift at this site. M_2 and M_1 are thought to correlate with Horizon M of the Blake-Bahama Basin (see Site 603 chapter). As discussed further in the Site 603 chapter, Vail et al. (1980) place Horizon M at the "basal middle Tortonian." This may refer to our local reflection Horizon M_2, which has been labeled Merlin by Mountain and Tucholke (1985). These authors find it to be a level, continuous reflector that commonly truncates underlying reflectors, and consider it to be of widespread, regional importance. The stratigraphic sequences at DSDP Sites 106 and 104 indicate an age within planktonic foraminifer Zone N14, which, at the time of Mountain and Tucholke's publication, was accorded an age of about 12 Ma (draft of paper by Berggren, Kent, Flynn, et al., 1985). While in press, the Berggren et al. time scale underwent considerable revision, so that when it was published, Zone N14 was assigned a considerably younger age of about 10.3 to 11.4 Ma, as shown in Figure 7 (from Berggren, Kent, Flynn, et al., 1985). As revised, N14 falls at the top of the middle Miocene where it overlaps the lower part of coccolith Zone CN6.

As Horizon M_2 (or Reflector Merlin) strongly truncates underlying reflectors at Site 603 (Fig. 3), it should be evidenced in the drilled sequence by a prominent hiatus. The nannofossil data (Fig. 6) would suggest correlation of M_2 with the sharp disconformity delineated between Zones CN6 and CN7b (between 660.8 and 672.0 m). It is interesting that a second hiatus is indicated some 30 m upsection from the first (between 632.0 and 641.6 m). This may correspond to the second parallel but equally strong reflection just a short distance (about 0.3 sec) above M_2.

If the above correlations are correct, then the age attributed to M_2 (or Merlin) here corresponds closely with that postulated elsewhere (taking into account the time scale revision mentioned above). Cores 39 to 41 were dated as foraminifer Zone N14 during a preliminary study aboard ship using planktonic foraminifers (Site 603 chapter). According to the published Berggren, Kent, Flynn, et al. (1985) time scale (Fig. 7), the overlap between N14 and nannofossil Zone CN6 would place a maximum age on the hiatus (and therefore on M_2/Merlin) of between 10.5 and 10.8 Ma. By the same token, foraminifer Zone N15 and the upper portion of CN6 should be missing, which does appear to be the case, as suggested previously by the nannofossil evidence and by the fact that N15 was not detected during the shipboard study. In addition, nannofossil Subzone CN7a is also missing (its top is not delineated in Fig. 7); thus the minimum date for the hiatus (M_2) falls somewhere within CN7 time (10.0 to about 8.8 Ma, presumably within the lower portion of the zonal interval). Thus at Site 603, the hiatus correlated with M_2 or Merlin has removed the lowermost upper Miocene (lowermost Tortonian) and perhaps slightly older sediment. This would have all been classified as middle Miocene sediment under the previous Berggren time scales, and that age is reflected in most of the pre-1986 literature.

Our interpretation above is not without some contradictions. The preliminary shipboard foraminiferal study also dates Cores 603-34 and 603-38 as NP14 on the basis of the overlap of rare *Globorotalia praemenardii* and *Globigerina nepenthes*. According to the Berggren, Kent, Flynn, et al. (1985) time scale, this is inconsistent with the nannofossil dates, since NP14 should not overlap Zones CN7 or CN8. One might argue that the rare *Globorotalia praemenardii* reported could have been reworked upward. This is possible, given that, in addition to erosion associated with the disconformities, sediment

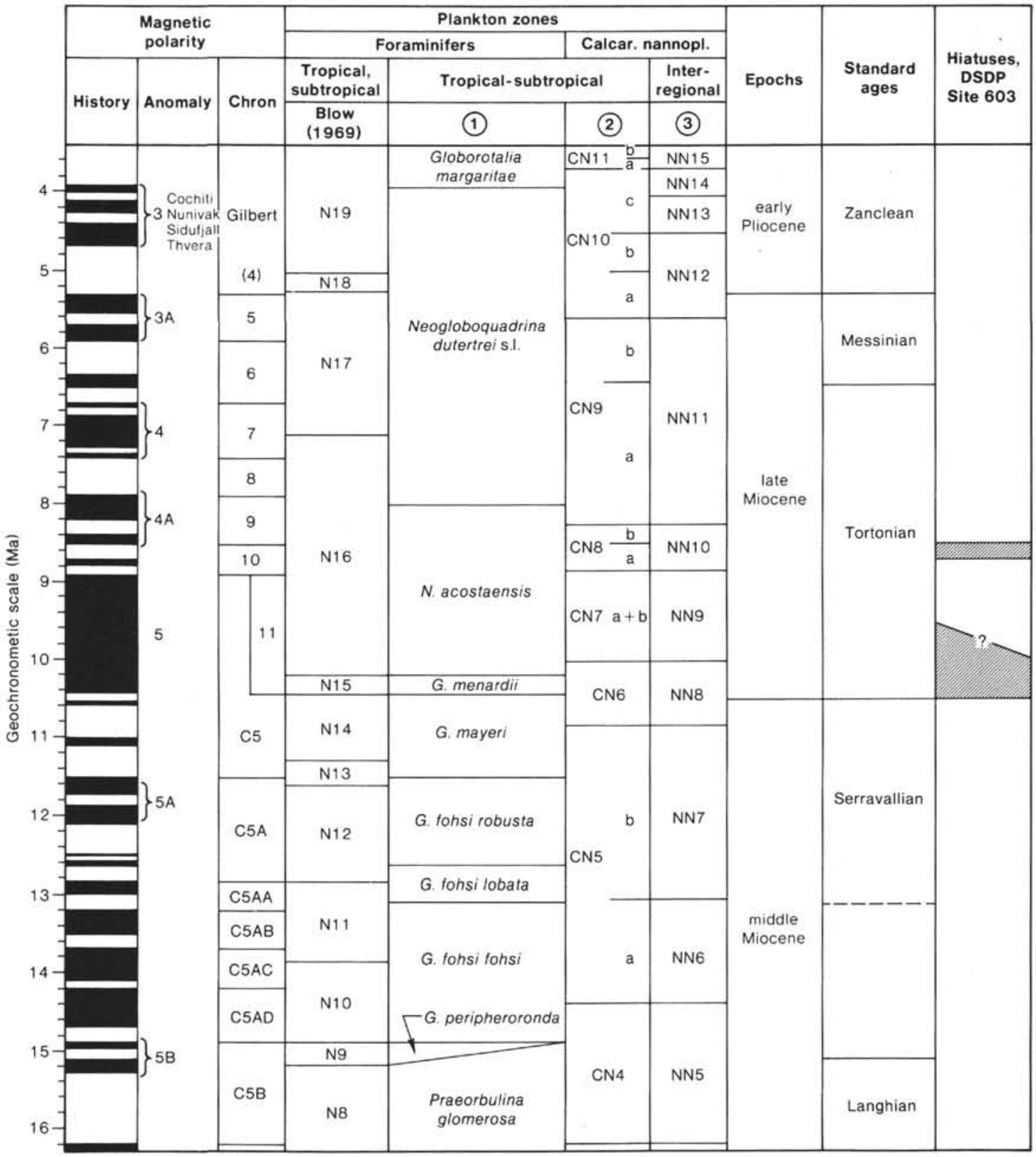

Figure 7. Portion of the Berggren et al. (1985) Neogene time scale used in this report (from Berggren, Kent, Flynn, et al., 1985, fig. 6). Shaded zones represent the hiatuses associated with local reflection Horizon M2 (=Merlin) and a superjacent parallel reflector at Site 603. Plankton zones indicated by circled numbers as follows: (1) after Bolli and Premoli-Silva (1973), Stainforth et al. (1975); (2) Bukry (1973, 1975), Okada and Bukry (1980); (3) Martini (1971).

wave deposition (indicative of a relatively strong bottom-current regime) began in this section a short distance beneath Reflector Merlin (Mountain and Tucholke, 1985 fig. 8-30 caption), and continued thereafter. Reworking, however, is not evident among the nannofloras. Perhaps further recalibration between the nannofossil and foraminiferal zones in this portion of the time scale will be necessary to resolve such discrepancies.

Other results within this volume that contradict our interpretation come from the correlation of reflection Horizon M_2 with other levels in the section, namely, at about 600 m (shipboard results given in the Site 603 chapter and in van Hinte et al., 1985) and at 563 m (Core 603-27) (Biart, this volume). These identifications were made, however, before the detailed nannofossil data were available. The shipboard identification of M_2 is interesting because it corresponds to a point where we see the hint of a possible hiatus at 600 m (Fig. 6). The sedimentation curve through that level, however, indicates no significant missing section, and we do not believe that the strongly erosive Reflector Merlin would correlate with a level so high in the section.

As previously stated, we observe no evidence in the way of disconformities to explain the presence of other reflection horizons above M_2/Merlin. The resolution of our zonation may not be sufficient to resolve any such hiatuses, if they are brief. The other reflections noted in Figure 3 may result from minor hiatuses or from subtle changes in physical properties (see discussions by Biart, this volume).

There are not observed in this section any hiatuses which would correspond to the regional seismic Reflector "Blue," which Mountain and Tucholke (1985) attribute to a second major pulse of intensified bottom water which eroded sediments over a broad area near the early/late Pliocene boundary, about the time Northern Hemisphere glaciation began. Ma'alouleh and Moullade (this volume) do see in the planktonic foraminiferal record significant cooling at about this time, but no discernable hiatus. Mountain and Tucholke (1985, fig. 8-30) trace Reflector Blue beneath the turbidite pond to the west of Site 603, but apparently not beneath the crest of the Hatteras Outer Ridge adjacent to our drill site (see further discussions of the evolution of the HOR in Wise et al. (in press) and Wise and van Hinte (this volume). It is not clear why a regional reflector such as Blue would be observed beneath the turbidite pond but not within the contourites of the HOR.

CORRELATION OF REFLECTION HORIZON MERLIN (M2) BETWEEN SITES 603 AND 604 (UPPER RISE OFF NEW JERSEY)

Nannofossil studies of the upper Miocene sequence drilled at Site 604 beneath the upper continental rise off New Jersey reveal a series of events complementary to those outlined in the present paper (Lang and Wise, this volume). There a spectacular lower Tortonian debris flow was penetrated 46 m before the hole had to be terminated short of reflection Horizon M_2 (=Merlin?). Lang and Wise assign the debris flow sediments recovered to Zones CN7 and CN8, which correspond precisely to the "condensed interval" associated with hiatuses at Site 603 (Fig. 6). The discontinuous debris flows are succeeded by a more continuous, 155-m claystone sequence dated from Zone CN9 (late Tortonian) well into the Plio-Pleistocene.

The debris flows at Site 604 indicate significant canyon cutting along the shelf, slope, and upper rise during the Vail et al. (1980) Cycle Tm3.1 sea-level drop, which Vail (1985, personal communication; Greenlee, et al., in press) now believe to have been the sharpest and most profound of the late Miocene (exceeding in magnitude that of the Messinian). Materials being cut from canyon walls along the shelf and slope began to accumulate at some point along the upper and lower rise and the abyssal plain beyond. The relative thinness at Site 603 of the CN7/CN8a sediments plus the hiatuses there suggest that a significant amount of these sediments either bypassed the site or, more likely, were subsequently eroded during times of intensified current activity. During nannofossil Zone CN8b time, however, the site apparently did lie within the locus of high net sediment accumulation for sediments eroded along the margin and passed through slope canyons, because the sedimentation rate reached the highest level documented for the site (192 m/Ma). This high sedimentation rate is comparable to that of the Miocene drift beneath the Blake Outer Ridge (160–180 m/Ma; Mountain and Tucholke, 1985).

A more complete description of the sequence in the vicinity of Site 604 is given by Wise et al. (1986), Lang and Wise (this volume), and Wise and van Hinte (this volume). The cause of the bottom-water pulse responsible for the disconformity associated with M_2 (Merlin) at both Sites 604 and 603, plus the subsequent erosion which continued until about CN9 time at Site 604 and at least the top of CN8a at Site 603, is a subject of considerable speculation. As discussed in more detail by Mountain and Tucholke (1985), Wise et al. (1986), and Lang and Wise (this volume), this event does not correspond with the climatic cooling associated with the formation of the East Antarctic Ice Cap, which occurs earlier (15–14 Ma). Using the now outdated time scale of Berggren et al. (prepublication version), Mountain and Tucholke (1985) dated Merlin at about 12 Ma, but noted that this was a time of climatic warming, not cooling. They suggested, therefore, that Merlin is probably not related to Antarctic glaciation, but rather some oceanographic or tectonic event—such as movement along the Greenland-Scotland Ridge—that would be peculiar to the North Atlantic. Such an event would allow a strong pulse of Arctic bottom waters to enter the North Atlantic, thus causing intensified bottom-current erosion. It is not clear, however, how such an abyssal event would cause canyon cutting along the shelf and slope where Merlin has also been well documented. Extensive erosion high on the margin could best be effected by lowered sea levels, which would be more easily envisioned if associated with known glacial activity.

The new Berggren et al. (1985) time scale and correlations used in the present paper date Reflector Merlin at Site 603 between about 9.6 and 10.5 Ma. We date its parallel subjacent reflector around 8.5 Ma. Debris flows at Site 604 presumably began at about the same time (Wise et al., 1986) and lasted at least as long, perhaps longer. This does place the timing of Merlin within the realm of glacial events associated with the formation of the West Antarctic Ice Sheet. As documented by Ciesielski and Weaver (1983; see also Wise et al., 1985), major abyssal erosion had begun as far north as the Falkland Plateau and beyond (DSDP Site 513) in the early late Miocene (prior to 9.5 or 10.0 Ma). This was followed by the initiation of ice rafting at these relatively lower latitudes (compared to the Antarctic continental margin) by 8.7 Ma, an event which Ciesielski and Weaver (1983) consider indicative of the establishment of large Antarctic ice shelves, which in turn probably led for the first time to the formation of a grounded West Antarctic Ice Sheet.[3]

All these major erosional and sedimentological events, in both the Antarctic and the North American basins, may have begun somewhat earlier than we have been able to date them, as indicated by the quartz sand turbidite bearing Eocene coccoliths in Sample 603B-6,CC. As discussed earlier, the turbidite would indicate that canyon cutting, or at least erosion of exposed outcrops,

[3] It should be noted that Ciesielski and Weaver's age dates are based on siliceous high-latitude microfossils correlated with the magnetic time scale by means independent of the Berggren et al. (1985) scale, which is based on low- to mid-latitude calcareous microfossils.

had occurred, perhaps on a limited scale, sometime between 13.0 and 10.8 Ma. The detection of turbidite as well as ice-rafting events is limited, of course, by the distance the observer's section is located from the source as well as by the magnitude of the events that caused them.

TAXONOMIC NOTES

Ceratolithus cristatus **Kamptner, 1950.** Bergen (1984), who sampled age-equivalent but contrasting diagenetic environments, presented convincing evidence that the ranges of *C. cristatus* and *C. rugosus* are identical and that these species are conspecific. We concur in that we observed *C. cristatus* in our section only where diagenetic overgrowths are minimal. The range of this taxon at Site 603 closely matched that reported for *C. rugosus*.

Discoaster misconceptus **(Theodoridis) Muza and Wise, n. comb.**

Basionym. *Eu-discoaster misconceptus* Theodoridis, 1984, p. 168-169, text figs. A-D, pl. 37, figs. 19, 20.

Discoaster quinqueramus **Gartner, 1969.** To pick the LO of *D. quinqueramus*, the species is distinguished by its optical continuity (seen best under crossed nicols using a gypsum plate) from broken specimens of *D. misconceptus* which have lost their terminal ray bifurcations. This latter form, formerly grouped with *D. pentaradiatus*, has recently been redescribed as a new species by Theodoridis (1984). The central knob or boss of *D. misconceptus* is also characteristically smaller (about a third the diameter of the central area or less). The central area boss in *D. quinqueramus* becomes progressively smaller up column, reaching a diameter about half that of the central area, at which point small specimens are difficult to distinguish from broken specimens of *D. misconceptus* which, through dissolution, are common near the Miocene/Pliocene boundary at Site 603.

Six-rayed discoasters. Discoasters in Hole 603C were separated into three taxonomic categories—*Discoaster brouweri, D. surculus*, and the *D. variabilis* group—because of the difficulty in consistently separating *D. variabilis, D. decorus*, and *D. challengeri* from each other. A further discussion of this is found in Backman and Shackleton (1983).

Gephyrocapsids. In this light microscope study, the FO of the *Gephyrocapsa* group cannot be adequately delineated, nor do we try to distinguish the various *Gephyrocapsa* species. As noted by Backman and Shackleton (1983), the morphometric work of Samtleben (1980) indicates that until further work of that kind is done, even the detailed taxonomic interrelationships of the gephyrocapsids cannot provide meaningful biostratigraphic information.

Reticulofenestrids. Throughout the section, reticulofenestrids are very abundant. The distinction between *Reticulofenestra pseudoumbilica* and the smaller 3-6-μm reticulofenestrids is based on the diameter of the placolith. Observation of the range in lengths of reticulofenestrids in this section has shown there to be a natural break between those reticulofenestrids with lengths in the 3-6-μm range and those that measure 8 μm or greater. Reticulofenestrids greater than 8 μm in this section are classified as *R. pseudoumbilica*, whereas those smaller than 8 μm are classified as *R. haqii* or *R. gelida*. This division places the LO of *R. pseudoumbilica* 12.6 m below the LOs of *Sphenolithus abies* and *S. neoabies*, which are synchronous in this section and are used in this paper to define the top of the *R. pseudoumbilica* Zone.

ACKNOWLEDGMENTS

We are pleased to acknowledge reviews of this paper by Drs. David Bukry (U.S. Minerals Management Service, La Jolla) and Thomas R. Worsley (Ohio University, Athens). We thank Mr. James A. Bergen (FSU) for providing handy "second opinions" on our identifications of various taxa. All of the detailed range charts were constructed by the first author, the micrographs were printed by Mrs. Gabrielle Li (FSU), and Mr. James R. Breza prepared the samples. Laboratory facilities were supported in part by NSF Grant DPP 84-14268 and by an equipment grant from the Amoco Foundation.

REFERENCES

Backman, J., and Shackleton, N. S., 1983. Quantitative biochronology of Pliocene and early Pleistocene calcareous nannofossils from the Atlantic, Indian, and Pacific oceans. *Mar. Micropaleontol.*, 8: 141-170.

Bergen, J. A., 1984. Calcareous nannoplankton from Deep Sea Drilling Project Leg 78A: evidence for imbricate underthrusting at the Lesser Antillian active margin. *In* Biju-Duval, B., Moore, J. C., et al., *Init. Repts. DSDP*, 78A: Washington (U.S. Govt. Printing Office), 411-445.

Berggren, W. A., Kent, D. V., Flynn, J. J., and Van Couvering, J. A., 1985. Cenozoic geochronology. *Geol. Soc. Am. Bull.*, 96:1407-1418.

Berggren, W. A., Kent, D. V., and Van Couvering, J. A., 1985. Neogene geochronology and chronostratigraphy. *In* Snelling, N. J. (Ed.), *Geochronology of the Geologic Record.* Geol. Soc., London, Mem., 10:211-260.

Blow, W. H., 1969. Late middle Eocene to Recent planktonic foraminiferal biostratigraphy. *Proc. 1st Int. Conf. Planktonic Microfossils*, Geneva (1967), 1:199-442.

Bolli, H. M., and Premoli-Silva, I., 1973. Oligocene to Recent planktonic foraminifera and stratigraphy of the Leg 15 Sites in the Caribbean Sea. *In* Edgar, N. T., Saunders, J. B., et al., *Init. Repts. DSDP*, 15: Washington (U.S. Govt. Printing Office), 475-497.

Bukry, D., 1973. Low-latitude coccolith biostratigraphic zonation. *In* Edgar, N. T., Saunders, J. B., et al., *Init. Repts. DSDP*, 15: Washington (U.S. Govt. Printing Office), 685-703.

_______, 1975. Coccolith and silicoflagellate stratigraphy, northwestern Pacific Ocean, Deep Sea Drilling Project, Leg 32. *In* Larson, R. L., Moberly, R., et al., *Init. Repts. DSDP*, 32: Washington (U.S. Govt. Printing Office), 677-692.

_______, 1985. Mid-Atlantic Ridge coccolith and silicoflagellate biostratigraphy, Deep Sea Drilling Project Sites 558 and 563. *In* Bougault, H., Cande, S. C., et al., Init. Repts. DSDP, 82: Washington (U.S. Govt. Printing Office), 591-603.

Ciesielski, P. F., and Weaver, F. M., 1983. Neogene and Quaternary paleoenvironmental history of Deep Sea Drilling Project Leg 71 sediments, Southwest Atlantic Ocean. *In* Ludwig, W. J., Krasheninnikov, V. A., et al., *Init. Repts. DSDP*, 71, Pt 2: Washington (U.S. Govt. Printing Office), 461-477.

Gartner, S., 1977. Calcareous nannofossil biostratigraphy and revised zonation of the Pleistocene. *Mar. Micropaleontol.*, 2:1-25.

Gartner, S., and Bukry, D., 1975. Morphology and phylogeny of the coccolithophycean family Ceratolithaceae. *J. Res. U.S. Geol. Surv.*, 3:451-465.

Gartner, S., Chen, M. P., and Stanton, R. S., 1984. Late Neogene nannofossil biostratigraphy and paleoceanography of the northeastern Gulf of Mexico and adjacent areas. *Mar. Micropaleontol.*, 8:17-50.

Greenlee, S. M., Schroeder, F. W., and Vail, P. R., in press. Seismic stratigraphic and geohistory analysis of Tertiary strata from the continental shelf off New Jersey—calculation of eustatic fluctuations from stratigraphic data. *Geol. Soc. Am.*

Haq, B. U., 1984. Jurassic to Recent nannofossil biochronology: an update. *In* Haq, B. U. (Ed.), *Nannofossil Biostratigraphy.* Benchmark Pap. Geol., 78:358-378.

Hay, W. W., 1970. Calcareous nannofossils from cores recovered on Leg 4. *In* Bader, R. G., Gerard, R. D., et al., *Init. Repts. DSDP*, 4: Washington (U.S. Govt. Printing Office), 455-501.

Heck, S. E. van, 1979a. Bibliography and taxa of calcareous nannoplankton. *Int. Nannoplankton Assoc. Newsl.*, 1:AB1-5, A1-12, B1-27.

_______, 1979b. Bibliography and taxa of calcareous nannoplankton. *Int. Nannoplankton Assoc. Newsl.*, 1:ABVI, A13-28, B28-42.

_______, 1980a. Bibliography and taxa of calcareous nannoplankton. *Int. Nannoplankton Assoc. Newsl.*, 2:5-34.

_______, 1980b. Bibliography and taxa of calcareous nannoplankton. *Int. Nannoplankton Assoc. Newsl.*, 2:43-81.

_______, 1981a. Bibliography and taxa of calcareous nannoplankton. *Int. Nannoplankton Assoc. Newsl.*, 3:4-41.

_______, 1981b. Bibliography and taxa of calcareous nannoplankton. *Int. Nannoplankton Assoc. Newsl.*, 3:51-86.

_______, 1982a. Bibliography and taxa of calcareous nannoplankton. *Int. Nannoplankton Assoc. Newsl.*, 4:7-50.

_______, 1982b. Bibliography and taxa of calcareous nannoplankton. *Int. Nannoplankton Assoc. Newsl.*, 4:65-96.

_______, 1983. Bibliography and taxa of calcareous nannoplankton. *Int. Nannoplankton Assoc. Newsl.*, 5:4-13.

Hinte, J. E. van, Wise, S. W., Biart, B. N. M., Covington, J. M., Dunn, D. A., Haggerty, J. A., Johns, M. W., Meyers, P. A., Moullade, M. R., Muza, J. P., Ogg, J. G., Okamura, M., Sarti, M., and von Rad, U., 1985. DSDP Site 603: first deep (>1000-m) penetration of the continental rise along the passive margin of eastern North America. *Geology*, 13:392-396.

Jansa, L. F., Tucholke, B. E., Gradstein, F. M., and Sheridan, R. E., 1979. Mesozoic-Cenozoic sedimentary formations of the North American Basin; western North American Basin. *In* Talwani, M., Hay, W. W., and Ryan, W. B. F. (Eds.), *Deep Drilling Results in the Atlantic Ocean: Continental Margins and Paleoenvironment.* Am. Geophys. Un., Maurice Ewing Ser., 3:1-57.

Kennett, J. P., and Srinivasan, M. S., 1983. *Neogene Planktonic Foraminifera: A Phylogenetic Atlas:* Stroudsburg, PA (Hutchinson Ross Publ. Co.).

Loeblich, A.R., Jr., and Tappan, H., 1966. Annotated index and bibliography of the calcareous nannoplankton. *Phycologia*, 5:81-216.

———, 1968. Annotated index and bibliography of the calcareous nannoplankton III. *J. Paleontol.*, 42:584-598.

———, 1969. Annotated index and bibliography of the calcareous nannoplankton III. *J. Paleontol.*, 43:568-588.

———, 1970a. Annotated index and bibliography of the calcareous nannoplankton IV. *J. Paleontol.*, 44:558-574.

———, 1970b. Annotated index and bibliography of the calcareous nannoplankton VI. *Phycologia*, 9:157-174.

———, 1971. Annotated index and bibliography of the calcareous nannoplankton VI. *Phycologia*, 10:315-339.

———, 1973. Annotated index and bibliography of the calcareous nannoplankton VII. *J. Paleontol.*, 47:715-759.

Lowrie, W., and Alvarez, W., 1981. One hundred million years of geomagnetic polarity history. *Geology*, 9:392-397.

Martini, E., 1971. Standard Tertiary and Quaternary calcareous nannoplankton zonation. *In* Farinacci, A. (Ed.), *Proc. II Plankt. Conf. Roma 1970* (Vol. 2): Rome (Edizioni Tecnoscienza), 739-785.

Martini, E., and Bramlette, M. N., 1963. Calcareous nannoplankton from the experimental Mohole drilling. *J. Paleontol.*, 37:845-856.

Mountain, G. S., and Tucholke, B. E., 1985. Mesozoic and Cenozoic stratigraphy of the United States Atlantic continental slope and rise. *In* Poag, C. W. (Ed.), *Geologic Evolution of the United States Atlantic Margin:* Stroudsburg, PA (Van Nostrand-Reinhold), pp. 293-341.

Okada, H., and Bukry, D., 1980. Supplementary modification and introduction of code numbers to the "Low-latitude coccolith biostratigraphic zonation" (Bukry, 1973; 1975). *Mar. Micropaleontol.*, 5:321-325.

Parker, M. E., Clark, M., and Wise, S. W., 1985. Calcareous nannofossils of Deep Sea Drilling Project Sites 558 and 563, North Atlantic Ocean: biostratigraphy and the distribution of Oligocene braarudosphaerids. *In* Bougault, H., Cande, S.C., et al., *Init. Repts. DSDP*, 82: Washington (U.S. Govt. Printing Office), 559-589.

Robb, J. M., Hampson, J. C., Jr., Kirby, J. R., and Twichell, D. C., 1981. Geology and potential hazards of the Continental Slope between Lindenkohl and South Toms Canyons offshore mid-Atlantic United States. *U.S. Geol. Surv. Open File-Rept.*, 81-600.

Robb, J. M., Hampson, J. C., Jr., and Kirby, J. R., 1982. Surficial geologic studies of the continental slope in the Northern Baltimore Canyon Trough area—techniques and findings. *Proc. 14th Ann. Offshore Tech. Conf., Houston, Texas*, Paper OTC 4170, pp. 39-43.

Samtleben, C., 1980. Die Evolution der Coccolithophoriden-Gattung *Gephyrocapsa* nach Befunden in Atlantik. *Palaeontol. Z.*, 54(1-2): 91-127.

Stainforth, R. M., Lamb, J. L., Luterbacher, H., Beard, J. H., and Jeffords, R. M., 1975. *Cenozoic Planktonic Foraminiferal Zonation and Characteristic Index Forms.* Univ. Kansas Paleontol. Contrib., Art. 62.

Steinmetz, J. C., 1985. Bibliography and taxa of calcareous nannoplankton-IV. *Int. Nannoplankton Assoc. Newsl.*, 7:23-26.

Theodoridis, S., 1984. *Calcareous Nannofossil Biozonation of the Miocene and Revision of the Helicoliths and Discoasters.* Utrecht Micropaleontol. Bull., 32.

Tucholke, B. E., and Laine, E. P., 1982. Neogene and Quaternary development of the lower continental rise off the current United States east coast. *In* Watkins, J. S., and Drake, C. (Eds.), *Studies in Continental Margin Geology.* Am. Assoc. Pet. Geol. Mem., 34:295-305.

Vail, P. R., Mitchum, R. M., Jr., Shipley, T. H., and Buffler, R. T., 1980. Unconformities of the North Atlantic. *R. Soc. London Phil. Trans.*, 294:137-155.

Wise, S. W., Gombos, A. M., and Muza, J. P., 1985. Cenozoic evolution of polar water masses, southwest Atlantic Ocean. *In* Hsü, K. J., and Weissert, H. J. (Eds.), *South Atlantic Paleoceanography:* Cambridge (Cambridge University Press), pp. 283-324.

Wise, S. W., Hinte, J. E. van, Mountain, G. S., Biart, B. N. M., Covington, J. M., Drugg, W. S., Dunn, D. A., Farre, J., Habib, D., Hart, M. B., Haggerty, J. S., Johns, M. W., Lang, T. H., Meyers, P. A., Miller, K. G., Moullade, M. R., Muza, J. P., Ogg, J. G., Okamura, M., Sarti, M., and von Rad, U., in press. Mesozoic-Cenozoic clastic depositional environments revealed by DSDP Leg 93 drilling on the continental rise off the eastern United States. *In* Summerhayes, C. P. (Ed.), *North Atlantic Palaeoceanography:* London (Blackwell Scientific Publications).

Date of Initial Receipt: 10 July 1985
Date of Acceptance: 9 May 1986

APPENDIX

Calcareous Nannofossils Considered in This Report, in Alphabetical Order of Species Epithets

Sphenolithus abies Deflandre, 1953
Discoaster asymmetricus Gartner, 1969
Discoaster barbadiensis Tan Sin Hok, 1927
Discoaster bellus Bukry and Percival, 1971
Discoaster berggrenii Bukry, 1971
Braarudosphaera bigelowii (Gran and Braarud) Deflandre, 1947
Zygrhablithus bijugatus (Deflandre) Deflandre, 1959
Reticulofenestra bisecta (Hay, Mohler, and Wade) Roth, 1970
Discoaster bollii Martini and Bramlette, 1963
Discoaster braarudii Bukry, 1971
Discoaster brouweri Tan, 1927
Discoaster burkei Black, 1971
Coccolithus formosus (Kamptner) Wise, 1973
Catinaster calyculus Martini and Bramlette, 1963
Helicosphaera carteri (Wallich) Kamptner, 1954
Discoaster challengeri Bramlette and Riedel, 1954
Catinaster coalitus Martini and Bramlette, 1963
Umbilicosphaera cricota (Gartner) Cohen and Reinhardt, 1968
Ceratolithus cristatus Kamptner, 1950
Reticulofenestra daviesii (Haq) Haq, 1971
Discoaster deflandrei Bramlette and Riedel, 1954
Amaurolithus delicatus Gartner and Bukry, 1975
Discoaster druggii Bramlette and Wilcoxon, 1967
Neococcolithes dubius (Deflandre) Black, 1967
Coccolithus eopelagicus (Bramlette and Riedel) Bramlette and Sullivan, 1961
Discoaster exilis Martini and Bramlette, 1963
Eiffelithus eximius (Stover) Perch-Nielsen, 1968
Coccolithus formosus (Kamptner) Wise, 1973
Cyclicargolithus floridanus (Roth and Hay) Bukry, 1971
Reticulofenestra gelida (Geitzenauer, 1972) Backman, 1978
Uniplanarius gothicus (Deflandre) Hattner and Wise *in* Wind and Wise, 1983
Discoaster hamatus Martini and Bramlette, 1963
Reticulofenestra haqii Backman 1978
Discoaster intercalaris Bukry, 1971
Pontosphaera japonica (Takayama) Burns, 1973
Discoaster kugleri Martini and Bramlette, 1963
Pseudoemiliania lacunosa (Kamptner) Gartner, 1969
Calcidiscus leptoporus (Murray and Blackman) Loeblich and Tappan, 1978
Discoaster loeblichii Bukry, 1971
Calcidiscus macintyrei (Bukry and Bramlette) Loeblich and Tappan, 1978
Discoaster misconceptus (Theodoridis), n. comb.
Sphenolithus moriformis (Bronnimann and Stradner) Bramlette and Wilcoxon (1967)
Pontosphaera multipora (Kamptner) Roth, 1970
Sphenolithus neoabies Bukry and Bramlette, 1969

Discoaster neohamatus Bukry and Bramlette, 1969
Discoaster neorectus Bukry, 1971a
Chiasmolithus oamaruensis (Deflandre) Stradner and Edwards, 1978
Coccolithus pelagicus (Wallich) Schiller, 1930
Discoaster pentaradiatus Tan, 1927
Discoaster prepentaradiatus Bukry, 1971
Amaurolithus primus (Bukry and Percival) Gartner and Bukry, 1975
Reticulofenestra pseudoumbilica (Gartner) Gartner, 1969
Pontosphaera pulcheroides (Sullivan) Romein, 1979
Discoaster quinqueramus Gartner, 1969
Isthmolithus recurvus Deflandre *in* Deflandre and Fert, 1954
Reticulofenestra reticulata (Gartner) Roth, 1973
Ceratolithus rugosus Bukry and Bramlette, 1968
Triquetrorhabdulus rugosus Bramlette and Wilcoxon, 1967
Discoaster saipanensis Bramlette and Riedel, 1954
Helicosphaera sellii (Bukry and Bramlette) Jafar and Martini, 1975
Discoaster surculus Martini and Bramlette, 1963
Discoaster tamalis Kamptner, 1967
Discoaster tani nodifer Bramlette and Riedel, 1954
Discoaster triradiatus Tan, 1927
Eiffellithus turriseiffeli (Deflandre and Fert) Reinhardt, 1965
Ceratolithus telesmus Norris, 1965
Reticulofenestra umbilica (Levin) Martini and Ritzkowski, 1968
Discoaster variabilis Martini and Bramlette, 1963

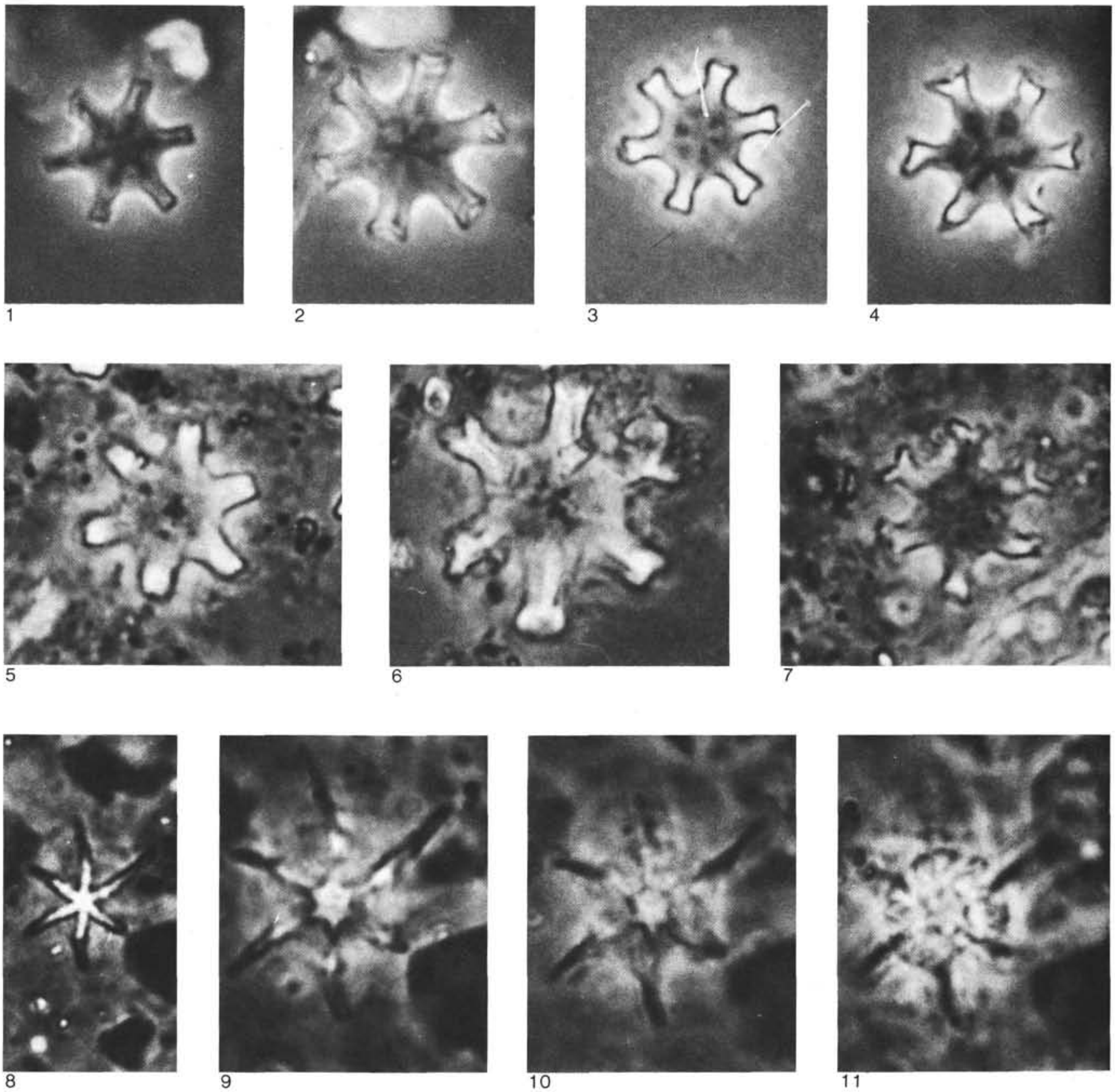

Plate 1. Middle Miocene nannofossils, phase contrast light micrographs. **1–7.** *Discoaster kugleri* Martini and Bramlette, ×2300, (1–4) topotype specimens, Sample Bo 355, Trinidad; note the variation in the ray terminations, which range from (1) nearly flat, to (2, 3), slightly knotched and enlarged to (4) clearly bifurcated; (5–7) Sample 603-51-1, 40 cm; note variations in ray terminations similar to those in the topotype material except that in the Hole 603 material these bifurcations appear even more pronounced. **8–11.** *Catinaster calyculus* Martini and Bramlette, Sample 603-38-1, 100–102 cm, (8) ×2350; (9–11) high to low focus, ×3500.